JOURNAL OF AEROSOL MEDICINE AND PULMONARY DRUG DELIVERY
Volume 30, Number 5, 2017

Pp. 299–321
DOI: 10.1089/jamp.2015.1286

Original Research

Development of Optimized, Inhalable, Gemcitabine-Loaded Gelatin Nanocarriers for Lung Cancer

Susanne R. Youngren-Ortiz, BSc, PhD,[1] David B. Hill, PhD,[2,3] Peter R. Hoffmann, PhD, MSPH,[4] Kenneth R. Morris, MS, PhD,[1,5] Edward G. Barrett, PhD,[6] M. Gregory Forest, PhD,[7] and Mahavir B. Chougule, BPharm, MPharm, PhD[1,8–10]

Abstract

Background: Aerosol delivery of chemotherapeutic nanocarriers represents a promising alternative for lung cancer therapy. This study optimized gemcitabine (Gem)-loaded gelatin nanocarriers (GNCs) cross-linked with genipin (Gem-GNCs) to evaluate their potential for nebulized lung cancer treatment.

Methods: Gem-GNCs were prepared by two-step desolvation and optimized through Taguchi design and characterized for physicochemical properties. Particle size and morphology were confirmed by scanning and transmission electron microscopy. *In vitro* release of Gem from Gem-GNCs performed in Dulbecco's phosphate-buffered saline and simulated lung fluid was evaluated to determine release mechanisms. Particle size stability was assessed under varying pH. Differential scanning calorimetry and powder X-ray diffraction were used to determine the presence and stability of Gem-GNC components and amorphization of Gem, respectively. Gem-GNC efficacy within A549 and H460 cells was evaluated using MTT assays. Mucus rheology upon treatment with Gem-GNCs, lactose, and normal saline control was measured. Andersen cascade impaction identified the aerodynamic particle size distribution of the nebulized formulation.

Results: Gem-GNCs had particle size, zeta potential, entrapment efficiency, and loading efficiency of 178 ± 7.1 nm, -18.9 mV, 92.5%, and 9.1%, respectively. The Gem and formulation excipients where molecularly dispersed and configured amorphously. Gem-GNCs were stable at pH 5.4–7.4 for 72 hours. Gem release from Gem-GNCs was governed by non-Fickian controlled release due to diffusion/erosion from a matrix-based nanocarrier. Gem-GNCs elicited a 40% reduction of the complex viscosity $\eta^*(1\,\text{Hz})$ of human bronchial epithelial cell mucus containing 3 wt% solids to mimic mild airway disease. The nebulized Gem-GNCs had a mass median aerodynamic diameter (MMAD) of $2.0 \pm 0.16\,\mu$m, geometric standard deviation (GSD) of 2.7 ± 0.16, and fine particle fraction (FPF) of $75.2\% \pm 2.4\%$. The Gem-GNC formulation did not outperform the Gem solution in A549 cells. However, in H460, Gem-GNCs outperformed the Gem IC50 reduction by $\sim$5-fold at 48 and 10-fold 72 hours.

[1]Translational Drug Delivery Research (TransDDR) Laboratory, Department of Pharmaceutical Sciences, The Daniel K. Inouye College of Pharmacy, University of Hawai'i at Hilo, Hilo, Hawai'i.
[2]Department of Physics and Astronomy, The University of North Carolina at Chapel Hill, Chapel Hill, North Carolina.
[3]Marsico Lung Institute/CF Center, The University of North Carolina School of Medicine, Chapel Hill, North Carolina.
[4]Department of Cell and Molecular Biology, John A. Burns School of Medicine, University of Hawai'i, Honolulu, Hawai'i.
[5]The Lachman Institute for Pharmaceutical Analysis, Arnold & Marie Schwartz College of Pharmacy and Health Sciences, Long Island University–Brooklyn Campus, Brooklyn, New York.
[6]Respiratory and Asthma Program, Lovelace Respiratory Research Institute, Albuquerque, New Mexico.
[7]Carolina Center for Interdisciplinary Applied Mathematics, The University of North Carolina at Chapel Hill, Chapel Hill, North Carolina.
[8]Pii Center for Pharmaceutical Technology, Research Institute of Pharmaceutical Sciences, University of Mississippi, Oxford, Mississippi.
[9]Translational Drug and Gene Delivery Research (TransDGDR) Laboratory, Department of Pharmaceutics and Drug Delivery, School of Pharmacy, University of Mississippi, Oxford, Mississippi.
[10]Natural Products and Experimental Therapeutics Program, University of Hawai'i Cancer Center, University of Hawai'i, Honolulu, Hawai'i.

Conclusion: Stable, effective, and sustained-release Gem-GNCs were developed. The nebulized Gem-GNCs had satisfactory MMAD, GSD, and FPF and the formulation reduced the dynamic complex viscosity of mucus consistent with increased mobility of nanoparticles.

Keywords: gelatin, gemcitabine, inhalation, lung cancer, nanoparticles, Taguchi factorial design

Introduction

DESPITE THE RECENT ADVANCES in diagnosis and treatment, lung cancer is the second most common cancer only trailing prostate cancer in men and breast cancer in women.[1] In the United States, lung cancer is the leading cause of cancer deaths with an estimated 158,000 deaths in 2015.[2,3] An estimated 221,200 new cases of lung cancer were diagnosed in 2015, accounting for ~13% of all cancer diagnoses.[3] The lung cancer 5-year survival rate for cases where the disease is still localized within the lungs is 54%; however, only 15% of lung cancer cases are diagnosed at an early stage.[4] For metastasized tumors, the 5-year survival rate is 4%.[4] The overall lung cancer survival rate is much lower than other leading cancers, 17.8%.[4]

Nonsmall cell lung cancer (NSCLC) occurs when malignant cells form in the tissues of the lung and can be classified as squamous cell carcinoma, large cell carcinoma, adenocarcinoma, pleomorphic, carcinoid tumor, salivary gland carcinoma, and unclassified carcinoma.[1] Approximately 85% of all lung cancers are identified as NSCLC, where 75% of these cases are metastatic at diagnosis.[5]

Standard treatment involves combinations of surgery, chemotherapy, and radiation therapy. Although early detection and treatment make a significant difference in life expectancy, the majority of patients diagnosed with lung cancer present with locally advanced or metastatic disease.[6] Current NSCLC anticancer drugs have poor tumor tissue selectivity and toxicity issues that contribute to their overall low efficacy and detrimental effects to normal tissues. Well-designed drug delivery systems that can deliver anticancer therapeutics to cancerous cells should be developed to avoid adverse effects and increase efficacy.

Approximately 90%–95% of all lung cancers originate in the airway epithelial cells of the lung.[7,8] NSCLC comprises a heterogeneous aggregate of at least three histological subtypes, including squamous cell carcinoma, adenocarcinoma, and large cell carcinoma. Squamous cell tumors are usually located in the bronchi.[9] Adenocarcinoma usually occurs in the periphery of lung tissue, including the terminal bronchioles and the alveoli.[10] A distinct variant of adenocarcinoma is mucinous cystadenocarcinoma of the lung, a rare malignant mucus-producing neoplasm caused from uncontrolled growth of transformed airway epithelial cells.[11] Large cell carcinoma is highly anaplastic, associated with rapid metastasis, therefore often occurring peripherally and spreading centrally in the lungs.[12]

Gemcitabine (Gem), 4-amino-1-(2-deoxy-2,2-difluoro-β-D-erythro-pentofuranosyl)pyrimidin-2(1H)-one hydrochloride (2′,2′-difluorodeoxycytidine), is a deoxycytidine analog that has been identified as a first-line treatment for NSCLC in combination with cisplatin.[13–15] The therapeutic potential of Gem in the treatment of cancer is hindered by its short plasma half-life (short infusions ranging from 30 to 90 minutes, long infusions 4–11 hours), poor metabolic stability, and fast elimination rate.[16] Gem is metabolized by cytidine deaminase following systemic administration to the inactive 2′-deoxy-2,2′-difluorouridine, which is then cleared by urinary excretion by the kidneys.

The tolerability of Gem is more favorable than other anticancer drugs such as cisplatin etoposide combinations in NSCLC patients; however, serious side effects, including myelosuppression, neutropenia, thrombocytopenia, and anemia, may occur.[17–19] The anticancer effects of Gem are dependent on high dosages (1000–1250 mg/m^2), requiring weekly administration of a prolonged infusion (30 minutes) to achieve therapeutic responses.[20]

Since Gem is a prodrug, it must first be transported into the cell through a nucleoside transporter, and then it must be phosphorylated by deoxycytidine kinase to become pharmacologically active. Gem cellular uptake requires active transporters due to its inability to enter cells by passive diffusion.[21,22] Since the uptake of Gem is mediated by both types of transporters, sodium independent and dependent, activity of these nucleoside transporters is fundamental to the inhibition of cell growth and essential for the clinical efficacy of the nucleoside analog.[23] This is supported through studies that have shown that nucleoside transporter deficiency or inhibition causes considerable resistance of tumor cells to Gem.[21,24] A new drug delivery system capable of efficient Gem delivery to its site of action may avoid the development of resistance and should overcome the limitations associated with transporter deficiency resistance.

Drug delivery through the inhalation route of administration has the ability of allowing a high extent of local absorption by taking advantage of the large surface area, thin alveolar epithelium, permeable membrane, and extensive vasculature.[25] Consequently, the use of local passive administration of an ideal inhalable lung cancer therapy to the tumor site allows for maximum therapeutic concentration of drug while maintaining lower adverse side effects associated with systemic administration.[26]

Administration by inhalation offers a noninvasive means to circumvent first-pass metabolism, reduce the therapeutic dose and frequency of administration, and deliver drugs directly to their site of action with increased local drug concentrations, thereby reducing the potential of systemic toxicity.[27] A safe and effective drug delivery system that releases drug in a sustained manner is desirable to limit exposure to normal tissues while delivering the active chemotherapeutic to the cancer cells.[28]

Nanocarriers represent a class of drug delivery systems with the potential to minimize degradation of therapeutic agents, prevent adverse side effects, and increase the availability of the drug at its intended site of action for therapeutic benefit. Administering a drug to the site of therapeutic action allows for generally lower doses to achieve clinically effective results. Therefore, nanocarriers should be engineered to slowly degrade, react to stimuli, and to be site specific.[29]

Nanocarrier formulations such as nanoliposomes, nanostructured lipid carriers, dendrimers, and polymeric nanoparticles have previously been used for targeting lung cancer.[30–35] Polymeric nanoparticles represent an interesting lung cancer-targeting platform because they may entrap drug and imaging agents and may also contain surface-targeting moieties for selective uptake within lung cancer cells or tissues.[36,37] The most commonly used polymers for lung cancer-targeting nanoparticles are polylactic acid, poly(ε-caprolactone), poly(lactide-*co*-glycolide) (PLGA), alginic acid, chitosan, and gelatin. Entrapping chemoagents within a polymeric nanoparticle allows for the chemotherapeutic agent to maintain the biodistribution pattern of the polymer, as opposed to conventional therapeutics. This allows for sustained release of drug and protects from degradation of the active pharmaceutical ingredient.[38]

Although inhalation delivery of chemotherapeutic nanomedicines offers great advantages in maintaining an enhanced local drug concentration for lung cancer treatment, inhaled nanocarriers encounter physiological barriers to their effective target site delivery. The airway barriers limit the distribution, penetration, and absorption of drugs within the lung and include mucus, mucociliary clearance, and macrophage uptake.

For effective lung cancer targeting through inhalation, a nanocarrier delivery system should obtain deposition and localization on the target area of the lung, have mucus-penetrating properties, have the ability to avoid mucociliary clearance, provide effective cellular uptake, and evade uptake by alveolar macrophages.[39–41] Once the nanoparticles deposit on the target location of the lung, it should traverse the mucus layer where it could come into contact with the tumor tissue. The enhanced permeability and retention (EPR) effect may play a role in the nanoparticle entrance and residence time within the tumor tissues due to poor lymphatic drainage.[42,43] Elicitation of the EPR effect may occur if the developed Gem-gelatin nanocarriers (GNCs) are capable of mucus penetration and evade macrophage clearance to reach the tumor tissues.

Gelatin is a biocompatible, biodegradable, and naturally derived polymer that elicits high physiological tolerance and low immunogenicity.[44] It is an FDA-approved polymer for oral, intravenous, and respiratory inhalation administration.[45] Gelatin possesses carboxyl and amine functional groups that allow for surface modification with targeting molecules or may be modified by the addition of varying levels of cross-linking agent to modify release characteristics.[44,46] There have been few studies on the development of gelatin nanoparticles containing chemotherapeutics for the local treatment of lung cancer by the inhalation route of administration.[47–49] Importantly, there have not been any previous studies that examine the formulation of a Gem-loaded GNC (Gem-GNC) for aerosol inhalation delivery. In this study, we have successfully prepared GNCs containing Gem and have characterized their physical and aerodynamic properties.

Nanocarriers with particle size hydrodynamic diameter of <200 nm may have increased uptake and action compared with larger particles with particle size of >200, possibly due to their ability to evade detection and removal by alveolar macrophages.[50] In addition, it was previously demonstrated that PEGylated nanoparticles with particle size of >100 and ≤200 nm were capable of penetrating respiratory mucus.[51] Hill et al. found that diffusive passage times through the mucus layer scale robustly with lung mucus weight percent solids.[40] Lung cancer causes decreased mucociliary clearance to suboptimal levels.[52] Additionally, the diffusion law of particles <200 nm in size is normal, whereas larger particles exhibit subdiffusion, and therefore the passage time distributions are far longer for larger particles. This also enhances the evasion of macrophages because the <200 nm particles traverse the mucus layer much faster.

Nanocarriers are difficult to deliver to the deep lung due to their inherent aerodynamic properties that inhibit deep lung deposition. To achieve nanocarrier deposition to the distal lung tissue, an appropriate pulmonary delivery device must be used such as a dry powder inhaler, metered dose inhaler, or nebulizer. We have designed a stable GNC hydrocolloid suspension for nebulization since studies have confirmed the stability of aerosolized gelatin particles.[47,53]

We hypothesized that the formulation of stable Gem-GNCs with particle size in the range of 150–200 nm will show controlled release of the Gem from the particles, exert improved anticancer effect, and effectively deliver to lungs upon nebulization. The objective of this study was to use Taguchi design of experiments to analyze how particle size is affected by the desolvating agent, the cross-linking agent, and the gelatin concentration. In this investigation, a Gem-GNC formulation, preserved in the lyophilized powder state, was designed to potentially be administered to the lungs through a nebulized nanosuspension following reconstitution. The GNCs were characterized for physicochemical and aerodynamic properties, as well as evaluated under cell-based assays.

Materials and Methods

Materials

Gelatin (type B; bloom strength of 225 g; isoelectric point of 4.7–5.2 [225 H 30 mesh Batch# 402101511]; Rousselot, Dubuque, IA) was a gift from the manufacturer. Genipin [methyl (1*R*,2*R*,6*S*)-2-hydroxy-9-(hydroxymethyl)-3-oxabicyclo[4.3.0]nona-4,8-diene-5-carboxylate] was a gift sample from Wilshire Technologies, Inc. (Princeton, NJ). Gem [4-amino-1-(2-deoxy-2,2-difluoro-β-D-erythro-pentofuranosyl)pyrimidin-2(1H)-one hydrochloride] was purchased from Sigma Chemicals (St. Louis, MO). Ethanol, dimethyl sulfoxide, 3-[4,5-dimethylthizol-2-yl]-2,5-diphenyl tetrazolium bromide (MTT), and lactose monohydrate were purchased from VWR International (Radnor, PA). Spectra/Por dialysis membrane (molecular weight cutoff [MWCO] of 25,000 Da) was obtained from Spectrum Laboratories, Inc. (Rancho Dominguez, CA).

All chemicals used were either analytical or tissue culture grade. All reagents and solvents were high-performance liquid chromatography (HPLC) or analytical grade. Distilled, deionized, 0.22 μm filtered sterile water was used throughout the experiments.

Cell culture

The NSCLC cell lines, A549 (ATCC® CCL-185™) and NCI-H460 [H460] (ATCC HTB-177™), were grown as monolayers in 75-cm^2 tissue culture flasks (Greiner Bio-One, Monroe, NC) at 37°C under 5% CO_2 in F12-K and RPMI supplemented

medium (Life Technologies, Grand Island, NY) with 10% fetal bovine serum (FBS) and an antibiotic–antimycotic solution of penicillin (5000 U/mL), streptomycin (0.1 mg/mL), and neomycin (0.2 mg/mL), respectively. Dulbecco's phosphate-buffered saline (DPBS) was purchased from Mediatech, Inc. (Manassas, VA). Cell culture media and penicillin/streptomycin/neomycin stock solutions were purchased from Cellgro (Herndon, VA). Heat-inactivated FBS was purchased from Atlanta Biologicals (Lawrenceville, GA).

Methods

Formulation and optimization of GNCs. For the preparation of GNCs, a two-step desolvation method was used, where the first step was the fractionation of gelatin to obtain the high-molecular-weight fraction with the use of bulk addition of antisolvent and the second step was the formation of the GNC by dropwise addition of nonsolvent. A schematic showing the formation process is outlined in Figure 1. To better understand the interrelationships between the dependent parameters and their optimization using a full factorial design is both time and labor-intensive.[54] Therefore, a Taguchi method with an L_9 orthogonal array design was selected to optimize the experimental conditions.

Preliminary trials were conducted to select factors and their working ranges that have major influence on the efficiency of the Gem-GNC formulation. The experimental range of gelatin concentration (% w/v), volume ratio of 90% v/v aqueous ethanol solution, and genipin concentration (% w/w) were found to be 0.5%–1.5% w/v, 7:10–9:10 v/v, and 0.2%–1.0% w/w, respectively. To minimize the number of trials necessary and to effectively study the effect of the factors in all possible combinations, a Taguchi orthogonal array design was utilized.

Type B anionic GNCs were prepared using the two-step desolvation technique with some modifications, followed by subsequent genipin cross-linking (Fig. 1).[55–57] Gem was added to each batch at a concentration of 1 mg/mL. The desolvating agent, ethanol, was added dropwise at a rate of ~2 mL per minute to the 0.5%, 1%, or 1.5% w/v gelatin solution at 40°C under constant stirring at 600 rpm, and the genipin solution (0.2%, 0.6%, or 1.0% w/w) was added dropwise (1 mL/min) immediately following the ethanolic solution addition. The solution was stirred at 600 rpm for an additional 60 minutes; at that point, the stirring rate and temperature were dropped to 200 rpm and 30°C, respectively, and allowed to stir until the ethanol had completely evaporated. The GNC colloidal suspension was corrected for volume with distilled deionized water at the process end stage. The particle size and zeta potential of the resultant GNCs in suspension were obtained by dynamic light scattering and electrophoretic mobility, respectively.

Taguchi orthogonal array method. In this study, gelatin concentration, volume ratio of desolvating agent (90% v/v aqueous ethanol) added to gelatin solution batch volume, and genipin concentration were selected as control factors and their levels were determined as shown in Table 1.[54,58] The concentration of gelatin was selected as the orthogonally distributed parameter. The orthogonal array (L_9, 3^3) was utilized to determine the optimal parameters and to analyze the effect of these parameters.[59] The formulation parameters were assigned to each column and nine combinations were formed as shown in Table 1.

The orthogonal array is configured in respect to the total degrees of freedom of the targeted function. The degrees of freedom (DF = 9–1 = 8) for L_9 orthogonal array can be equal to or more than the determined process parameters. The particle size error values were measured through the experimental design for each combination of control factors. The determination of the quality characteristics of the measured control factors was done by signal-to-noise (S/N) ratios, as shown in Figure 2B, where the lowest S/N ratios were inferred to have better quality. Formulation parameter selection was based on the target particle size of 150 nm and the regression analysis of the Taguchi dataset.

Taguchi S/N ratio was calculated for the particle size responses to understand the effect of the gelatin concentration, volume ratio of desolvating agent (90% v/v aqueous ethanol) added to gelatin solution batch volume, and genipin concentration factor levels on the particle size response (Fig. 2B). A higher S/N ratio infers higher influence of the parameter on the particle size. The S/N ratios were analyzed under the nominal is best condition, dependent on the target particle size of 150 nm. The S/N ratio was calculated using equation 1 as follows:

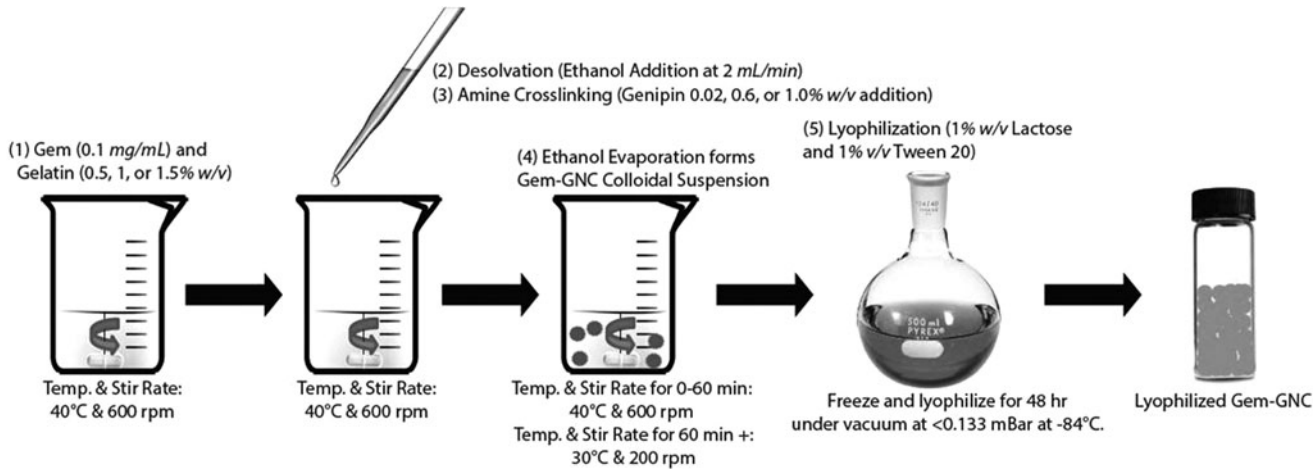

FIG. 1. Schematic showing the formulation of Gem-GNC. Gem-GNC, gemcitabine-loaded gelatin nanocarrier.

Table 1. Experimental Matrix and Responses From the L_9 Orthogonal Array and the Signal-To-Noise Ratios of Experimental Results for Particle Size of the Taguchi Orthogonal Array Gemcitabine Gelatin Nanocarrier Batches

	Formulation parameter level					
Batch no.	*Gelatin (% w/v)*	*v:v 90% v/v ethanol addition: batch volume*	*Genipin (% w/w)*	*Average particle size (nm)*	*Standard deviation of particle size (nm)*	*S/N (η_i, i = 1–9) (dB)*
1	0.5	7:10	0.2	155.2	42.16	−43.72
2	1	7:10	0.6	167.03	21.93	−46.89
3	1.5	7:10	1	559.67	300.89	−53.64
4	1	8:10	0.2	292.73	72.71	−47.43
5	1.5	8:10	0.6	355.37	208.63	−51.6
6	0.5	8:10	1	357.73	104.36	−53.7
7	1.5	9:10	0.2	156.77	68.44	−46.81
8	0.5	9:10	0.6	250.6	99.07	−46.33
9	1	9:10	1	365.5	243.67	−52.08

Particle size was determined with PBS, pH 7.4, at 25°C by dynamic light scattering as described within the Methods section. The gelatin concentration was expressed as a weight volume percent (% w/v) of gelatin weight to batch volume. The desolvating agent addition was expressed as volume ratio of 90% v/v ethanolic aqueous solution to volume of gelatin batch. The genipin concentration was expressed as weight percent (% w/w) of genipin to gelatin weight. Experiments were performed in triplicate ($n = 3$).

dB, decibels; S/N, signal-to-noise.

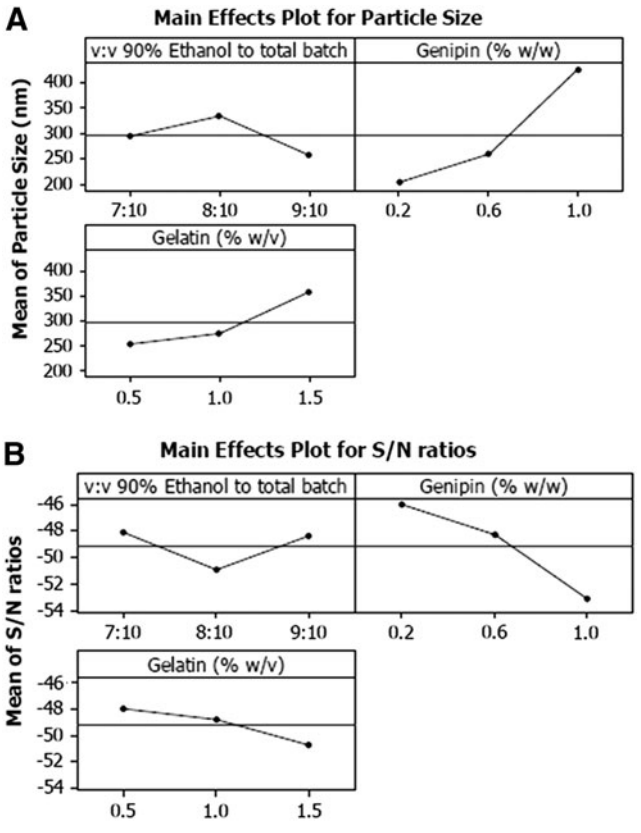

FIG. 2. Experimental analysis of Taguchi designed experiments: **(A)** Taguchi main effects plot for mean particle size and **(B)** main effects plot for particle size S/N ratios of Gem-GNC batches. The three-leveled parameters within the designed experiments were the volume ratio (v:v) of 90% ethanol to total batch volume, genipin weight to gelatin percent (% w/w), and gelatin weight to batch percent volume (% w/v). The largest variation of the S/N ratio of the genipin concentration suggests that it has the largest influence on the particle size. S/N, signal-to-noise.

$$\textit{Nominal is best}: \frac{S}{N} = 10 \times \log\left(\frac{\bar{Y}^2}{\sigma^2}\right) \quad (1)$$

where $\bar{Y}$ is the response mean and σ is the variance. The nominal is best was applied because a targeted response of 150 nm particle size was desired. The relative influence of each factor level was determined by comparing S/N ratios of the particle size. This analysis determines which factor has more effect on the particle size by finding the largest range of the S/N ratio.

Preparation and purification of Gem-GNC. Following the same method as described above, Gem (1 mg/mL) was added to the 10 mL gelatin solution before the dropwise desolvating ethanol addition. The resultant GNCs were purified by one cycle of centrifugation at 10,000 *g* for 30 minutes to remove any crystallized Gem, followed by dialysis against PBS pH 7.4 using a 12–14 kDa dialysis membrane for 1 hour with three medium changes (Spectrum Laboratories, Inc.). Then, 1% w/v lactose monohydrate and 1% v/v Tween 20 (CRODA, Inc., Columbus, NJ) were used as a cryoprotectant and surfactant, respectively, and the batch was frozen to −80°C for 3 hours. The frozen Gem-GNC suspension was lyophilized for 48 hours under vacuum at <0.133 mBar at −84°C using a Freezone 12 Plus lyophilizer (Labconco, Kansas City, MO).

The Gem-GNC formulation suspension for nebulization was prepared by resuspending the lyophilized formulation in deionized water for *in vitro* characterization. The formulation, as prepared, will be reconstituted in 0.9% normal saline solution and administered as a suspension through the inhalation route of administration.

Particle size and zeta potential before and after lyophilization. The particle size of the prepared Gem-GNC was determined by dynamic light scattering using an NICOMP ZLS 380 analyzer (PSS-NICOMP, Santa Barbara, CA).[60,61] Particle sizes of the GNC and GEM-GNC were assessed by dispersion in PBS pH 7.4. The zeta (ζ) potential was assessed

by dispersion in distilled deionized water containing sodium chloride (1 μM) and was placed into the photoelectric cell. The movement of the liposomes in response to the electric field allows for the calculation of their electric charge. The ζ potential was determined by the electrophoretic mobility (μ) measurements. The mobility μ of the nanoliposomes at 25°C was converted to ζ potential by the Smoluchowski equation:

$$\zeta \text{ potential} = \frac{\mu\eta}{\varepsilon}$$

where η is the viscosity of the dispersion solvent and ε is the permittivity of the solution.[62,63] For each batch, at least three independent samples were taken and each was recorded in triplicate ($n = 3$).

Surface morphology and particle size through scanning electron microscopy and transmission electron microscopy. Micrograph images of the Gem-GNCs were obtained with a Hitachi S-4800 field emission scanning electron microscope with an Oxford INCA X-Act EDS System and a 120 kV Hitachi HT7700 transmission electron microscope (Chiyoda, Tokyo, Japan). The fully digital transmission electron microscopy (TEM) was outfitted with a video camera for fast scanning and alignment and an AMT XR-41 2048 × 2048 pixel bottom-mount camera for high-resolution imaging. The microscope was equipped with a high-tilt stage for electron tomography.

Analytical quantification of Gem using HPLC. HPLC analysis of Gem was performed with a Dionex Ultimate 3000 LC system, including a pump, autosampler, column compartment, and diode array detector, and data were displayed on the Chromeleon 7 software (Dionex, Sunnyvale, CA). Samples were isocratically eluted using a reverse-phase HPLC system (Dionex) with a C18 column (Phenomenex, Inc., Torrance, CA). We adapted and modified an HPLC method for Gem quantification.[64] Methanol and water (30:70, v/v) containing 0.01 M ammonium acetate (NH_4OAc) were used as the mobile phase and detection was performed at a wavelength of 268 nm.

Determination of Gem entrapment and loading efficiency. The entrapment efficiencies of Gem within the Gem-GNC formulations were determined by employing Vivaspin500 ultracentrifuge filters with an MWCO of 10 kDa (Viva Products, Inc., Littleton, MA) using HPLC with UV spectrophotometry to quantify the free Gem in the sample. Briefly, Gem-loaded formulations (0.5 mL) were placed on top of the Vivaspin filters and centrifuged at 16,200 *g* for 15 minutes. The aqueous filtrate generated at the bottom of the Vivaspin 500 ultracentrifuge tubes was then subjected to HPLC analysis in triplicate ($n = 3$), as described above, to determine the concentration of unloaded Gem ($\lambda_{max} = 268$ nm). The entrapment efficiency of the Gem within the developed formulation was calculated using equation 2 as follows:

$$\textit{Entrapment Efficiency } (EE),\ \% = \frac{X_1 - X_2}{X_1} \times 100\% \quad (2)$$

where X_1 = amount of total Gem initially added to the batch, normalized to sample size (mg), and X_2 = amount of free Gem detected after ultracentrifugation (mg).

Loading efficiency (LE) of Gem within the GNC was calculated with the following equation 3:

$$\textit{Loading Efficiency } (LE),\ \% = \frac{X_1 - X_2}{\textit{Total mass GNC } (mg)} \times 100\% \quad (3)$$

where X_1 = total mass of Gem initially added to the batch, normalized to sample size (mg), and X_2 = mass of free Gem detected after filtration centrifugation (mg).

In vitro release of Gem from Gem-GNC. The *in vitro* release of Gem from the developed formulation was assessed under physiological pH employing DPBS, pH 7.4, and within Gamble's solution to simulate the interstitial conditions within the lung as release media. Gamble's solution was prepared by dissolving the following within distilled deionized Milli-Q water (g/L): 0.095 magnesium chloride, 6.019 sodium chloride, 0.298 potassium chloride, 0.126 disodium hydrogen phosphate, 0.063 sodium sulfate, 0.368 calcium chloride dihydrate, 0.574 sodium acetate, 2.604 sodium hydrogen carbonate, and 0.097 sodium citrate dihydrate.[65]

Briefly, 2 mL of Gem-GNC formulation was placed inside a dialysis bag (MWCO12-14 kDa; Spectrum Laboratories, Inc.). The membrane bags were placed in 100 mL of DPBS (pH 7.4) under constant agitation at 200 rpm at 37°C ± 2°C. At predetermined time intervals (0, 0.5, 1, 2, 3, 4, 5, 6, 7, 8, 24, 48, 72 hours), 1 mL of dissolution medium was collected with equal volume of fresh dissolution medium while maintaining sink conditions. Each formulation underwent release studies using three independent release vessels. The samples were analyzed at each time interval in triplicate ($n = 3$) using the HPLC method described earlier. The time versus percent Gem release was plotted to evaluate the release profile of the developed formulation. *In vitro* release of Gem from Gem-GNC and Gem solution within DPBS and Gamble's simulated lung fluid (SLF) were analyzed using the free open-source software, KinetDS 3 rev 2010, available at http://sourceforge.net/projects.kinetds/[66]

pH stability of Gem-GNC. Since tumor interstitial tissues and cells have acidic pH, it was necessary to measure the influence of pH on the particle size and zeta potential as stability markers of the Gem-GNC at pH 5.4–7.4.[54] The Gem-GNC was incubated in DPBS pH 5.4, 6.4, and 7.4 up to 72 hours to assess the influence of pH on the surface charge and size of the nanoformulations as indicators of stability. Samples were collected and analyzed in triplicate ($n = 3$) every 24 hours.

Differential scanning calorimetry. The physical state of Gem within the gelatin matrix was evaluated using a TGA/DSC1 (METTLER TOLEDO, Columbus, OH). Approximately 2 mg of the Gem-GNCs, GNC placebo with Gen cross-linker, and lactose monohydrate as cryoprotectant with and without Gem present outside the NCs were used. Genipin, Gem, and lactose monohydrate were weighed into an aluminum pan, hermetically sealed, pan lids were pinholed to allow for escape of any volatile components, and the sample was analyzed over the range of −10°C to 260°C at a heating rate of 10°C min^{-1}. Transition temperatures

were determined from the endothermic or exothermic peak minima, while transition enthalpies were obtained by integration of endothermic transitions using linear baselines.

Placebo GNCs were prepared by the same process as the Gem-GNC samples, but prepared without the addition of the active ingredient Gem. The physical mixture of placebo GNC and Gem was prepared in the same way, except that 100 mg of Gem was dissolved within the suspending agent before freezing and lyophilization.

Powder X-ray diffraction. X-ray diffraction (XRD) measurements of Gem-GNC, GNC placebo with genipin crosslinker, and lactose monohydrate as cryoprotectant with and without free Gem outside the NCs, placebo GNC noncrosslinked with unentrapped genipin and Gem, and Gem alone were conducted to compare their crystalline structure using a Bruker D8 Advance powder XRD diffractometer (AXS GmbH, Karlsruhe, Germany) over an angular range of 5°–50°. The powder XRD (PXRD) instrument is equipped with a vertical goniometer in the Bragg–Brentano geometry (θ–2θ). The signal was conditioned using a Gobel mirror and collected using LYNXEYE linear detector. A Cu-Kα radiation source was used, and the scanning (*2*) rate was 5°/min.

Approximately 0.25 g of powder sample was filled into a low background Si crystal cut on the 511 plane sample cell and gently compressed with a glass slide to make the sample surface and holder surface coplanar. The divergence slit was 0.1 mm, with a step size of 0.01 and scan speed of 0.5 seconds per step. The Gem-GNC, placebo-GNC, and type 2 gelatin were placed in a regular sample holder. The powder diffraction patterns of the various Gem-GNCs, placebo GNC controls, and the individual excipient controls were analyzed for crystalline or amorphous characteristics by identifying the presence of large diffracted peaks or an amorphous halo.

In vitro aerosol characterization. Aerodynamic particle size distribution was measured using an 8-stage nonviable Andersen cascade impactor (Westech Scientific Instruments, Marietta, GA) lined with plates on each stage and an end-stage filter. To prevent particle bounce during nebulization, each plate on the impactor was coated with polysorbate 20 (Tween 20). A compressor nebulizer, the Vios® Aerosol Delivery system (PARI Respiratory Equipment, Inc., Midlothian, VA), was operated at a flow rate of 8 L/min and equipped with a Pari LC Sprint Nebulizer cup. The freeze-dried Gem-GNCs were redispersed in normal saline solution to a concentration of 50 mg/mL, which corresponded to a Gem dose of 100 μg/mL. The Gem-GNC formulation was nebulized for 10 minutes into the cascade impactor at a flow rate of 28.3 L/min after nebulization, the amount of formulation deposited on the throat, impactor stages (0–7), and filter was collected by washing with 2 mL of PBS pH 7.4. Samples were obtained and particles sized with the Nicomp 380ZLS as described above.

The nebulization process did not affect the particle size and surface charge of the GNCs, as shown by the insignificant change in these properties before and after nebulization. Then, the remaining samples underwent degradation experiments as follows. Samples from each plate that potentially contained Gem-GNCs were dispersed in 2 mL of trypsin solution (0.025 g/mL) in a 10-mL volumetric flask, shaken, and incubated at 37°C until a transparent solution formed ($\sim$10 minutes), indicating that complete digestion of the GNCs and release of all Gem encapsulated within the gelatin matrix had been achieved. Water was added to the flask and the solution was made up to volume and filtered through a 0.22-μm filter. The amount of Gem in the supernatant was analyzed using a validated HPLC, as discussed in a previous section, with a diode array UV absorbance detector (Ultimate 3000; Dionex).

The mass median aerodynamic diameter (MMAD), geometric standard deviation (GSD), and fine particle fraction (FPF) were obtained from impactor data using Microsoft Excel with appropriate formulas. The MMAD is the diameter at which 50% of the particles by mass are larger and 50% are smaller. The United States Pharmacopeia (USP) chapter <601> instructs to determine the MMAD by plotting the percentages of mass less than the stated aerodynamic diameters versus the aerodynamic diameters on log probability article. The MMAD is the intersection of the line with the 50% cumulative percent. GSD is a measure of the spread of an aerodynamic particle size distribution and is calculated using equation 4 as follows:

$$GSD = \left(\frac{d_{84}}{d_{16}}\right)^{\frac{1}{2}} \tag{4}$$

where d_{84} and d_{16} represent the diameters at which 84% and 16% of the aerosol mass are contained in diameters less than these diameters, respectively. The fraction of a dose that will deposit in the lung, because of its size, is known as the FPF. This is resembled by the portion of the mass that enters the impactor with an aerodynamic diameter smaller than 5 μm, defined as the FPF or respirable fraction ($FPF_{<5\ \mu m}$).[67] The optimal size for central airway deposition that represents the upper limit used to define this fraction varies between 4 and 6 μm, where particles of size 2–4 μm maintain peak peripheral lung deposition. There is no lower limit for FPF, although particles with sizes of less than 1 μm may be exhaled without deposition.[68]

The aerodynamic particle size distribution measurement is based on the amount of Gem deposited on each stage of the cascade impactor and represents a relative particle distribution. Respirable mass and respirable fractions were calculated from the known amount of drug deposited on the various parts. Only droplets measuring less than 5 μm in aerodynamic diameter were included in the assessment of the respirable mass and fraction. All cascade impactor experiments were repeated in triplicate ($n = 3$) and data are represented as mean ± SD.

Mucus rheology of Gem-GNC-treated mucus. Cystic fibrosis cell culture mucus was treated with DNase and PSA-DNases for 15 minutes, and changes in rheological properties were measured with a Bohlin Gemini rheometer using a 20 mm parallel plate geometry as previously described.[69,70] Briefly, the linear regime of a 1 Hz stress sweep was identified for each treatment condition. One hertz was the selected frequency for stress sweeps as it falls in-between the characteristic frequencies of tidal breathing ($\sim$0.25 Hz) and mucociliary clearance (10–15 Hz) and has been shown to correlate with mucociliary clearance.[71]

Mucus for all assays was harvested from human bronchial epithelial cell cultures as previously described[40,70] and prepared to 3 wt% solids to mimic a concentration that typifies mild airway disease.[40,72] Both Gem-GNCs and lactose were suspended in 0.9% NaCl with 10 mM EDTA and 0.01% sodium azide at 50 and 40 mg/mL, respectively. Once suspended, 6 μL of compound was added to 54 μL of 3% human bronchial epithelial (HBE) mucus for a final concentration of 5 mg/mL Gem-GNCs and 4 mg/mL lactose. Samples were allowed to incubate for 2 hours at 37°C.

Cell proliferation MTT assay. The effect of Gem-GNCs on the viability of A549 and H460 cell lines was measured using the established MTT assay protocol.[73] Briefly, A549 and H460 cells were seeded onto separate 96-well plates at a density of 5000 cells/well and incubated overnight. Cells were then treated with varying dosing levels of Gem-GNCs, placebo GNCs, and Gem solution ($n=4$) for 24, 48, and 72 hours. The 96-well plates were incubated at 37°C ± 0.2°C, and the cell viability was measured using the MTT assay.[74] Untreated cells were used as a control. Cell viability was plotted versus concentration of Gem and dose of Gem-GNCs.

Statistical analysis. One-way analysis of variance (ANOVA) with Tukey's multiple comparison post-test was used in the analysis of differences between the physicochemical properties of nanocarrier formulations. The least significant difference *post hoc* ANOVA was used in the comparison of particle sizes between different formulations. The experiments were conducted in triplicate with data reported as mean ± SD. The significance level was set at $p<0.05$. Statistical analysis was performed using Minitab 16 Statistical Software (State College, Benton, PA).

Results

Preparation and purification of Gem-GNC

The Taguchi method L_9-type orthogonal array design was used to optimize formulation parameters. The independent factors were the gelatin concentration (0.5, 1.0, and 1.5% w/v), volume ratio of 90% v/v aqueous ethanol to gelatin solution batch volume (7:10, 8:10, and 9:10 v:v), and genipin to gelatin weight percent (0.2, 0.6, and 1.0% w/w). The key dependent factor that was measured was particle size (nm). The S/N ratio was calculated for the particle size response to establish significance of each factor and their optimum levels for the optimized formulation. S/N ratios of particle size are shown in Table 1. The responses were interpreted by considering nominal S/N ratios for better accuracy of the measured data.

As shown in Table 1, the formulation parameters, A: gelatin (% w/v), B: volume ratio v:v of 90% v/v aqueous ethanol, and C: genipin (% w/w), were discriminated by considering different levels and possible effects according to the selected orthogonal array. The main effects plot was drawn for each factor at different levels by taking levels as x-coordinates and S/N ratios as y-coordinates (Fig. 2A, B). The plots show the effects of the individual factors on multiple responses in terms of their S/N ratios. Genipin concentration was inferred to be the most influential parameter on particle size since it has the largest S/N ratio range.

The predictive equations generated through linear regression for particle size are given in equation 5.

$$\begin{aligned} &\textit{Particle size } (nm) = \\ &\quad 169 - 1.82\ (\textit{volume ratio of } 90\%\ \textit{ethanol}) \\ &\quad + 283\ (\textit{Genipin } \%w/w) + 103(\textit{Gelatin } \%\ w/v) \end{aligned} \tag{5}$$

where R^2 coefficient of determination values for the particle size were calculated as 85.9%.

The target particle size value was 150 nm, so the volume ratio of 90% v/v ethanol was selected by fixing the gelatin and genipin concentrations to 1% w/v and 0.02% w/w, respectively. This led to the theoretical optimized parameter levels of 1.0% w/v gelatin to total batch volume, 7:10 v:v of 90% v/v aqueous ethanol to gelatin solution volume, and 0.2% w/w genipin to gelatin weight%. These levels were selected for further evaluation based on the Taguchi orthogonal array design and analysis.

Preparation and evaluation of lyophilized Gem-GNC

As shown in Table 2, the Gem-GNC average particle size was 166 ± 6.7 nm before lyophilization and 178 ± 7.1 nm after lyophilization. The zeta potential of the Gem-GNC formulation remained unchanged ($p>0.05$) before and after lyophilization and corresponded to –9.15 ± 0.45 mV and –9.07 ± 0.49 mV, respectively. In addition, the EE% and LE% of the Gem-GNC formulation were unaffected by the lyophilization process, as inferred by the insignificant ($p>0.05$) change from 93.7% to 92.5% and 9.2% to 9.1%, respectively. The placebo GNC had an average particle size of 152 ± 7.8 nm before lyophilization and of 167 ± 7.9 nm after lyophilization.

Table 2. Gemcitabine Gelatin Nanocarrier Particle Size, Zeta Potential, Entrapment Efficiency, and Loading Efficiency

Formulation	*Characterization parameters*	*Before lyophilization*	*After lyophilization (with reconstitution in water)*
Gem-GNC	Particle size (nm)	166 ± 6.7	178 ± 7.1
	Zeta potential (mV)	–9.15 ± 0.45	–9.07 ± 0.49
	EE%	93.7 ± 2.3	92.5 ± 2.5
	LE%	9.2 ± 0.4	9.1 ± 0.3
Placebo GNC	Particle size (nm)	152 ± 7.8	167 ± 7.9
	Zeta potential (mV)	–10 ± 0.51	–9.8 ± 0.56

EE, entrapment efficiency; Gem-GNC, gemcitabine-loaded gelatin nanocarrier; LE, loading efficiency.

The difference of particle size, zeta potential, EE%, and LE% before and after lyophilization was not statistically significant ($p > 0.05$) and the final reconstituted particle size was within our critical parameter of particle size <200 nm. The process validation batches ($n = 3$) had no significant differences between batches. Therefore, the formulation process was considered successfully robust at preparing stable Gem-GNCs.

Gem-GNC stability

The stability of the Gem-GNC was assessed in the presence of varying pH DPBS solutions (pH 5.4, 6.4, and 7.4). Figure 3A shows the particle size of the Gem-GNC formulations when in DPBS solutions of varying pH over the time points of 0, 1, 2, and 3 days. Particle size at the initial time point and at day 1 differs significantly ($p < 0.05$) from days 2 and 3 due to apparent GNC matrix erosion occurring between days 1 and 2. The polydispersity indices (PDIs) of the Gem-GNCs within the buffers at pH 5.4, 6.4, and 7.4 were not statistically significantly different (Fig. 3B). These nonsignificant differences in particle size and PDI of the Gem-GNC within varying pHs infer stability over varying pHs within a biologically relevant medium and a possible release mechanism of the Gem-GNC.

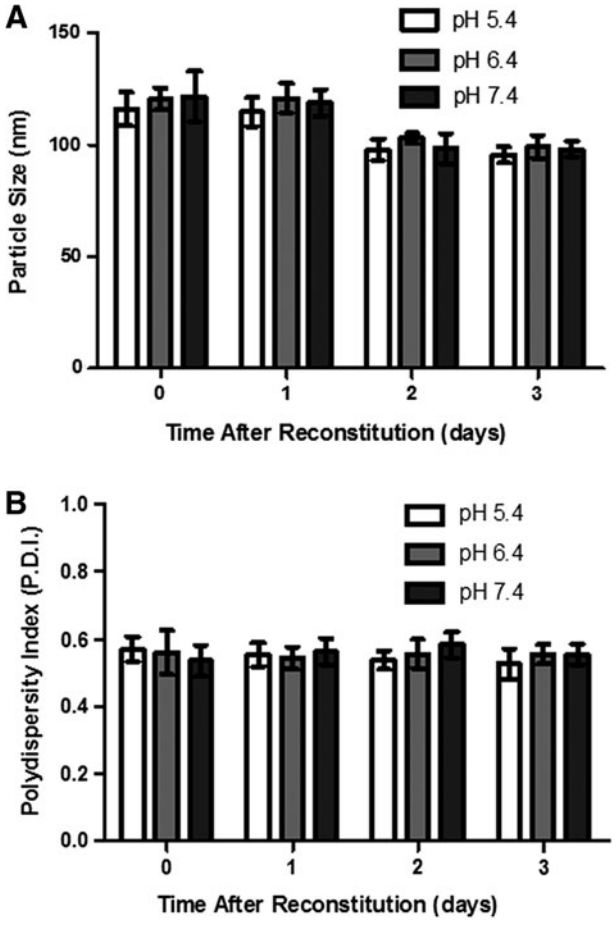

FIG. 3. Stability of Gem-GNC at pH 5.4, 6.4, and 7.4 in DPBS as assessed by the **(A)** particle size and **(B)** polydispersity index after reconstitution of the three independent Gem-GNC batches. Time after reconstitution of 0 days refers to 1 hour after rehydration with normal saline solution. Results are shown as mean ± SD ($n = 3$). Statistical significance was determined at $p < 0.05$. DPBS, Dulbecco's phosphate-buffered saline.

In vitro *release from Gem-GNC*

The Gem release profile within DPBS pH 7.4 and Gamble's simulated lung fluid (pH 7.4) of the Gem-GNC and Gem solution are shown in Figure 4. The Gem solution in both release mediums shows a rapid release that achieved 100% release in <6 hours. The Gem-GNC formulation displayed a sustained release of entrapped Gem, suggesting that the formulation had efficient retention and entrapment. The Gem-GNC showed ~20% release at 5 hours compared with the total release of the Gem solution at the same time. The release of the Gem-GNC at 24–72 hours showed a controlled release and attained 65% release by 72 hours.

When compared with the Gem release from Gem-GNCs within the DPBS alone, the release of Gem from Gem-GNCs within Gamble's simulated lung fluid initially exhibited a similar rate of release that progressed to faster and more overall release at 72 hours. At 72 hours, the Gem-GNC within Gamble's SLF achieved 81% release, as shown in Figure 4.

Drug release kinetics were assumed to be governed by diffusion within a matrix system.[75,76] Therefore, the release kinetics of the Gem from the Gem-GNCs were confirmed by fitting the release data into five kinetic models: zero order, first order, Weibull, Higuchi, and Korsmeyer–Peppas models.[77,78] The Gem-GNC release in DPBS and

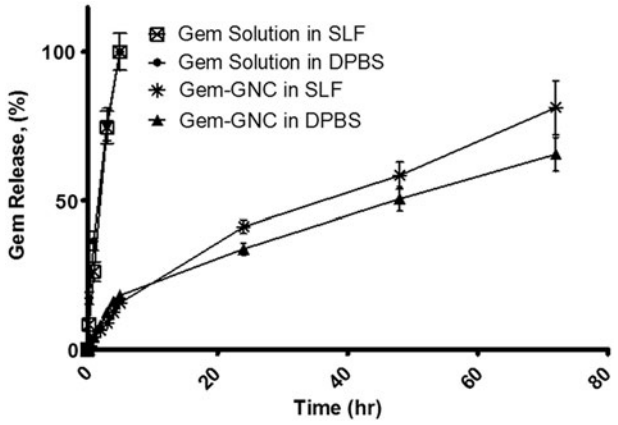

FIG. 4. *In vitro* release of Gem solution and Gem-GNCs within DPBS (pH 7.4) and SLF (Gamble's solution; pH 7.4). Lyophilized formulations were resuspended in distilled deionized water and placed into a dialysis membrane bag with molecular weight cutoff of 12–14 kDa. The membrane bags were then placed into 100 mL of DPBS or Gamble's SLF medium maintained at a temperature of 37°C with continuous stirring at 300 rpm. At specified time intervals, 0.5 mL dissolution medium was sampled and analyzed for Gem content using high-performance liquid chromatography with a UV diode array detector. The amount of Gem-GNC filled into the membrane bag was 10 mg/mL at 0.48% w/w Gem content. The Gem solution filled into the membrane bag was 0.1 mg/mL. Total volume of the Gem-GNC suspension and the Gem solution was 0.5 mL. Results are represented as mean ± SD ($n = 3$). SLF, simulated lung fluid.

TABLE 3. *IN VITRO* RELEASE MODELS SHOWING CORRELATION COEFFICIENT (R^2) VALUES FOR GEMCITABINE RELEASE FROM THE GEMCITABINE-GELATIN NANOCARRIERS WITHIN DULBECCO'S PHOSPHATE-BUFFERED SALINE AND SIMULATED LUNG FLUID (PH 7.4)

Model name	*Model*	*DPBS (pH 7.4) release medium* R^2	*SLF (pH 7.4) release medium* R^2
Zero order	$C_t = C_0 + K_0 t$	0.967	0.980
First order	$\log C = \log C_0 - \frac{Kt}{2.303}$	0.743	0.807
Higuchi	$f_t = Q = A\sqrt{D(2C - 2C2)Cs * t}$	0.972	0.994
Weibull	$M = M_0\left[1 - e^{\frac{-(t-T)^b}{\alpha}}\right]$	0.977	0.825
Korsmeyer–Peppas	$\frac{M_t}{M_\infty} = Kt^n$	0.964	0.993

Where K_0 is the zero-order release constant expressed in units of concentration/time, C_0 is the initial concentration of drug, K is the first-order rate constant, t is time, C is the initial drug concentration, Cs is the drug solubility in the matrix media, and D is the diffusivity of drug molecules (diffusion coefficient) in the matrix substance. M is the amount of drug dissolved as a function of time t, M_0 is total amount of drug being released, T accounts for lag time measured as a result of the dissolution process, a denotes a scale parameter that describes the time dependence, and b describes the shape of the dissolution curve progression. M_t/M_∞ is a fraction of drug released at time t, k is the release rate constant, and n is the release exponent.

DPBS, Dulbecco's phosphate-buffered saline; SLF, simulated lung fluid.

SLF media were fitted to these models and their respective R^2 values are presented in Table 3.

For release within the DPBS (pH 7.4) medium, the Weibull, Higuchi, and Korsmeyer–Peppas models were observed to have the best fit of the release profile with R^2 values of 0.977, 0.972, and 0.964, respectively. This indicated a matrix diffusion-based release. Release of Gem from the Gem-GNCs within Gamble's SLF had best fit with the Weibull and Korsmeyer–Peppas models that had corresponding R^2 values of 0.994 and 0.993, respectively. The Korsmeyer–Peppas power law was used to determine the drug release mechanism.[79] An exponent value of 0–0.5 indicates Fickian diffusion, while a value of 0.5 to <1 indicates non-Fickian diffusion release. In this study, the n values of 0.58 and 0.69 within the DPBS and Gamble's SLF suggest a non-Fickian mode of release due to diffusion and erosion mechanisms. This study confirmed that the mechanism of release is mixed diffusion and erosion from a matrix-based GNC.

Gem-GNC imaging with scanning electron microscopy and TEM

The scanning electron microscopy (SEM) and TEM micrographs of the Gem-GNCs are shown in Figure 5A and B, respectively. The SEM images show the Gem-GNC morphology, indicating that the particles have a smooth surface. The number mean particle size observed within the SEM micrograph was calculated as 229 ± 68 nm ($n = 7$). The number mean particle size calculated using the TEM micrograph was 197 ± 18 nm ($n = 6$). The particles appeared spherical within both the SEM and TEM images and the particle sizes corresponded to the average particle sizes and PDIs found with dynamic light scattering.

Differential scanning calorimetry

Differential scanning calorimetry (DSC) was performed on lyophilized samples of physical mixture of excipients, Gem-GNCs, and placebo GNCs to evaluate the thermal behavior of the sample to assess the physical state of Gem within the nanoparticle matrix. The endothermic events

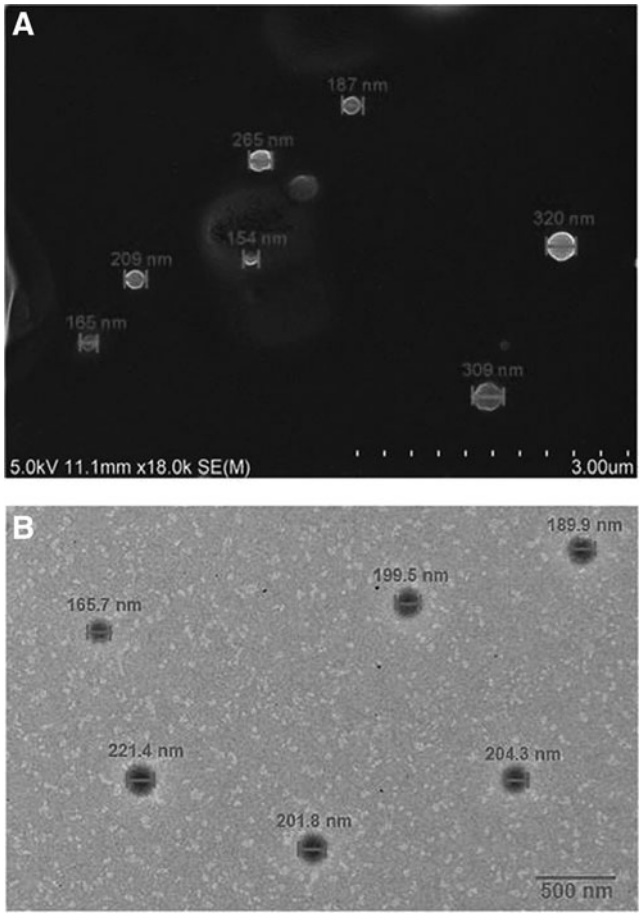

FIG. 5. SEM and TEM micrographs of the Gem-GNCs. **(A)** SEM micrograph with a scale bar of 3.0 μm and **(B)** TEM micrograph with a scale bar of 500 nm. The Gem-GNC particle size measured from the SEM micrograph is 229 ± 68 nm, while the particle size measured from this TEM micrograph is 197 ± 18 nm. SEM: HV = 5.0 kV. TEM: 0.002427 μm/pixel, HV = 100.0 kV, direct magnification 6000×. SEM, scanning electron microscopy; TEM, transmission electron microscopy.

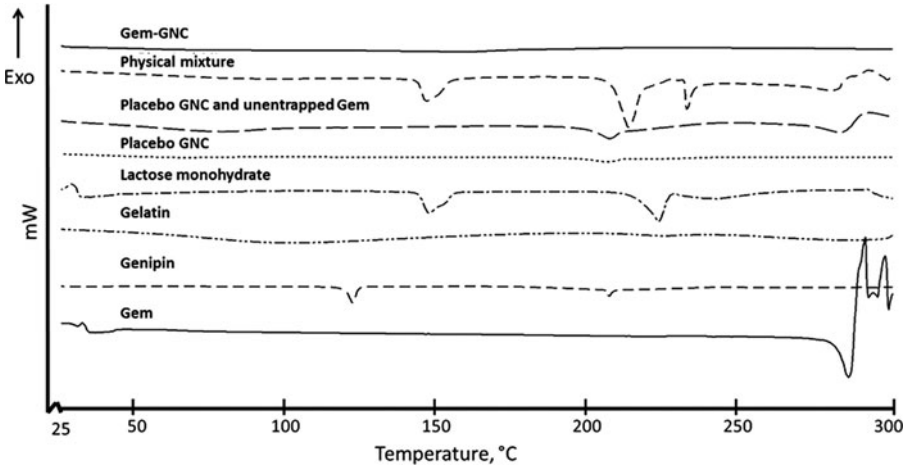

FIG. 6. Differential scanning calorimetry thermograms of the Gem-GNCs, physical mixture of actives and excipients, placebo GNCs and unentrapped Gem, placebo GNCs, lactose monohydrate, gelatin, genipin, and the active ingredient Gem. The samples were placed into the pinholed 40 μL aluminum crucibles, sealed, and the change of heat flux was analyzed with increasing temperature from 25°C to 300°C compared with an empty control crucible.

shown in Figure 6 are outlined in Table 4. The thermogram of Gem shows an endothermic peak at 290°C that correlates with literature values of 292°C for Gem melting point and degradation (Fig. 6).[80] The thermogram for the Gem-GNC shows no corresponding endotherm for Gem. The physical mixture had three endothermic events with onsets and peaks at 143.8°C and 150.2°C, 205.4°C and 211.2°C, and 231.4°C and 234.2°C (Fig. 6), respectively. The physical mixture (Fig. 6) also exhibited one exothermic degradation event with an onset temperature of 293.4°C preceded by an endothermic inflection consistent with melting of Gem. The endothermic peaks at 151.2°C and 223.6°C are attributed to lactose monohydrate and genipin in the physical mixture.

The lactose monohydrate thermogram had two endothermic events with onset temperatures of 143.5°C and 224.9°C and peak temperatures of 143.6°C and 226.0°C consistent with literature values for α-lactose monohydrate.[81] The placebo GNC and Gem mixture had one endothermic event at an onset temperature of 223.9°C and peak of 224.1°C that can be associated with lactose monohydrate and a melting and degradation event at an onset temperature of 292.1°C and peak of 300°C that was associated with the Gem. The placebo GNC alone displayed one endothermic event with an onset temperature of 219.7°C and peak of 220.4°C that may be attributed to the lactose monohydrate cryoprotectant. Genipin had two endothermic events with onset temperatures of 122.5°C and 207.8°C and peak temperatures of 122.7°C and 208.6°C. The endotherm at 122.5°C corresponds to genipin crystal form I as described previously.[82]

Gelatin exhibited broad endothermic peak onset at 50°C –75°C that occurred due to the release of water.[83] The Gem-GNC thermogram also did not show any endothermic or exothermic properties in this temperature range, indicating that the Gem and formulation excipients were molecularly dispersed.

Powder X-ray diffraction

To investigate the degree of order of the GNC matrix-associated Gem, the diffraction patterns of Gem, the lyophilized physical mixture of formulation constituents, lyophilized placebo GNCs, and lyophilized Gem-GNCs were obtained (Fig. 7). The PXRD pattern of Gem showed peaks that were sharp and intense, indicating its crystalline state (Fig. 7). The Gem-GNCs showed few sharp peaks of low intensities. The Gem and the physical mixture of the formulation components exhibited more crystallinity, whereas the lyophilized Gem-GNCs and placebo-GNCs showed amorphous or molecularly

TABLE 4. DIFFERENTIAL SCANNING CALORIMETRY DETERMINATION OF ENDOTHERMIC EVENTS OF THE GEMCITABINE GELATIN NANOCARRIERS, PHYSICAL MIXTURE OF ACTIVES AND EXCIPIENTS, PLACEBO GELATIN NANOCARRIERS AND UNENTRAPPED GEMCITABINE, PLACEBO GELATIN NANOCARRIERS, LACTOSE MONOHYDRATE, GELATIN, GENIPIN, AND THE ACTIVE INGREDIENT GEMCITABINE

	Tg (°C)	*Endothermic onset (°C)*	*Endothermic peak (°C)*	*Tm (°C)*
Gem-GNC	75	-	—	—
Physical mixture	—	143.8, 205.4, 231.4	150.2, 211.2, 234.2	293.4
Placebo GNC with unentrapped Gem	—	223.9	224.1	292.1
Placebo GNC	—	219.7	220.4	—
Lactose monohydrate	—	143.5, 224.9	143.6, 226	—
Gelatin	—	50	75	—
Genipin	—	122.5, 207.8	122.7, 208.6	—
Gem	—	—	—	290

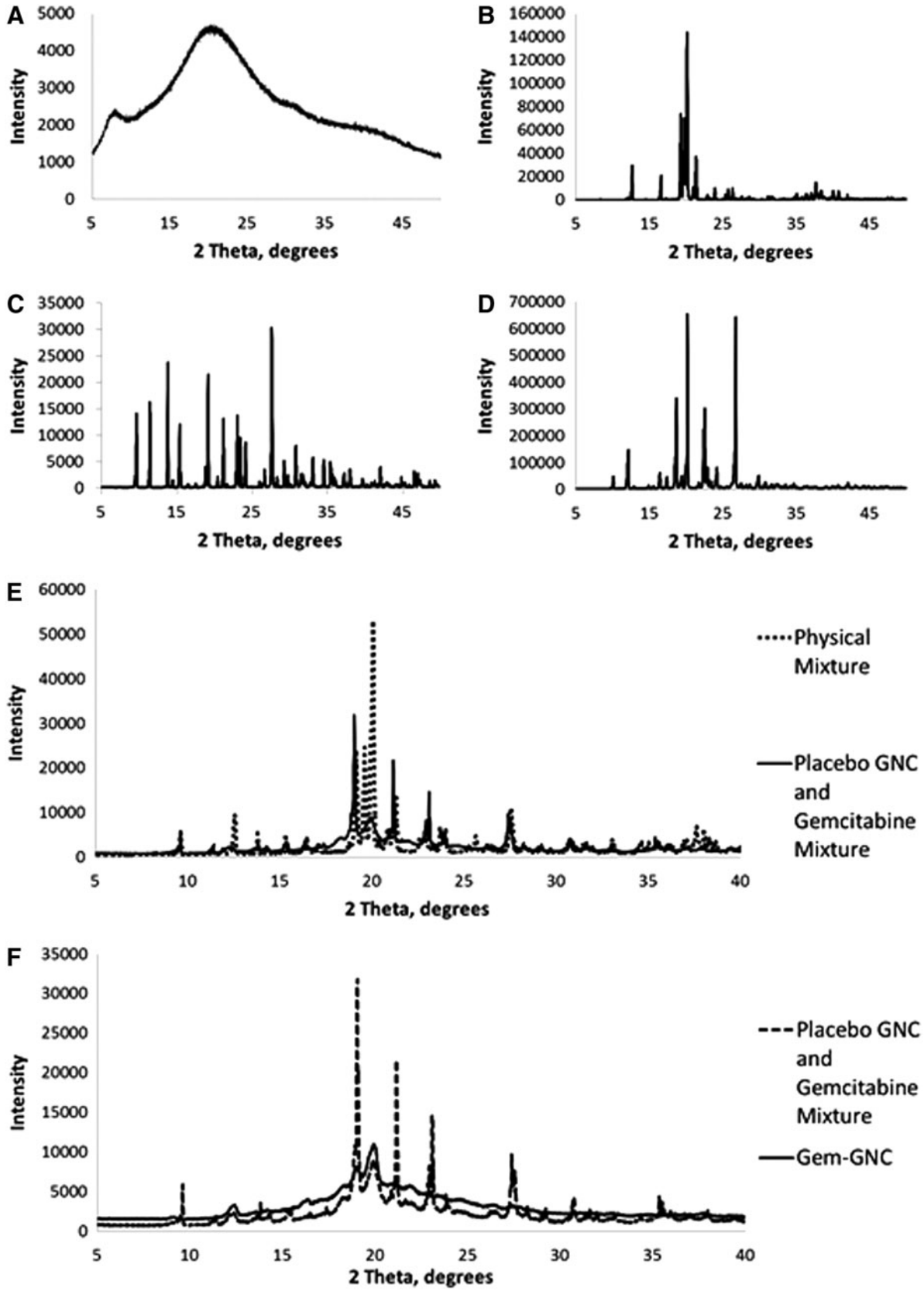

FIG. 7. Powder X-ray diffraction patterns. **(A)** Gelatin, **(B)** lactose monohydrate, **(C)** physical mixture of actives and excipients compared with the placebo GNC and Gem, **(D)** Gem, **(E)** genipin, and **(F)** Gem-GNC compared with the placebo GNC and Gem mixture.

dispersed properties. This confirmed that Gem within Gem-GNCs is amorphous.

Cell viability MTT assay

The results of the MTT cell viability assay of the A549 and H460 cells treated with Gem-GNCs and Gem solution are shown in Figure 8. Although A549 cells treated with Gem-GNCs did not achieve 50% cell kill after 48 hours, an IC_{50} of 0.013 and 0.023 μM after treatment with Gem solution and Gem-GNCs at 72 hours was observed, respectively. The Gem solution achieved IC_{50} values of 230 μM after 48 hours and 59 μM after 72 hours in treated H460 cells. H460 cells treated with the Gem-GNC formulation significantly outperformed the Gem solution, corresponding to IC_{50} values of 41 μM after 48 hours ($p < 0.01$) and 5.7 μM after 72 hours ($p < 0.01$). The H460 cells following 48 hours of treatment with Gem-GNCs had a 5-fold lower IC_{50} value than with the Gem solution ($p < 0.01$), whereas at 72 hours, the Gem-GNCs had a 10-fold lower IC_{50} value than the Gem solution ($p < 0.01$).

In vitro *aerosol characterization*

The Gem-GNC formulation was nebulized into an Andersen Mark-II cascade impactor. The stage number preseparator, 0, 1, 2, 3, 4, 5, 6, and 7 had the cutoff diameters of 10, 9, 5.8, 4.7, 3.3, 2.1, 1.1, 0.7, and 0.4, respectively. The

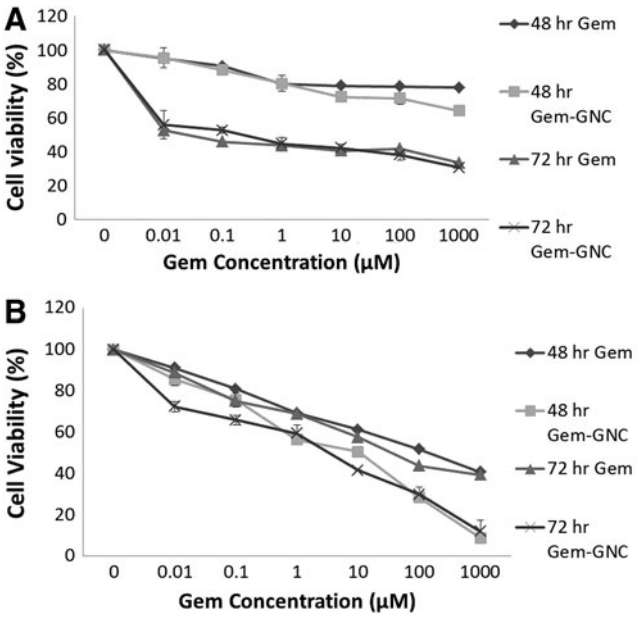

FIG. 8. Cell viability over time and concentration of A549 cells **(A)** and NCI-H460 cells **(B)** treated with Gem-GNC and Gem solution. Nontreated cells were used as controls. A549 cells treated with Gem-GNC had an IC_{50} value of 0.023 μM after 72 hours, whereas the Gem solution had an IC_{50} of 0.013 μM. The H460 cells treated with the Gem solution achieved IC_{50} values of 230 μM after 48 hours and 59 μM after 72 hours. H460 cells treated with the Gem-GNC formulation outperformed the Gem solution, corresponding to IC_{50} values of 41 μM after 48 hours ($p < 0.01$) and 5.7 μM at 72 hours ($p < 0.01$). Results are shown as mean ± SD ($n = 3$).

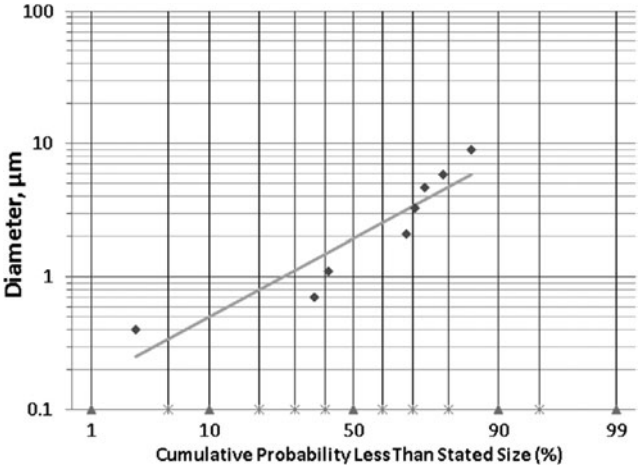

FIG. 9. Log cumulative probability plot of particle size versus cumulative weight percent (%) frequency of Gem-GNC impaction within an 8-stage nonviable Andersen cascade impactor. Data markers represent particle diameter (μm) of the nebulized nanocarrier containing droplets at a given cumulative probability less than stated size and the line is the best fit linear curve.

average net weight of Gem on each of the preseparator, stages 0–7, and filter was 0.31 ± 0.04, 0.81 ± 0.1, 0.59 ± 0.2, 0.46 ± 0.1, 0.51 ± 0.5, 0.71 ± 0.8, 2.3 ± 0.1, 0.5 ± 0.4, 2.6 ± 0.3, and 0.18 ± 0.04 μg, respectively. Particle size plotted against cumulative weight percent frequency of Gem-GNC impaction on the cascade impactor stages are shown in Figure 9. The total average emitted dose was 26.9 ± 2.4 μg calculated from three different cascade impactor runs. The Gem-GNC formulation showed an average MMAD of 1.99 ± 0.16 μm, GSD of 2.7 ± 0.16, and FPF of 76%.

Mucus rheology of Gem-GNC-treated mucus

The Gem-GNC particles reduced the complex viscosity η^* at 1 Hz of a 3 wt% human bronchial epithelial mucus sample by 40% from 0.12 to 0.71 Pa.s, as shown in Figure 10. This drop in η^* is consistent with a higher

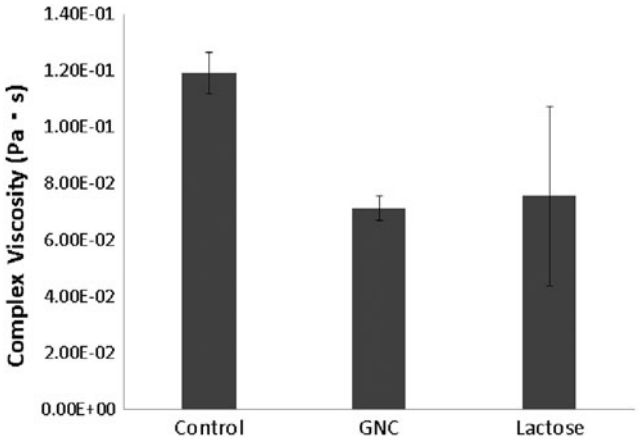

FIG. 10. Complex viscosity of 3% HBE mucus treated with 1:10 volume ratio of control buffer (0.9% NaCl, 10 mM EDTA, 0.01% sodium azide), 50 mg/mL GNC (Gem-GNC), and 40 mg/mL lactose. Results are shown as mean ± SD ($n = 3$). HBE, human bronchial epithelial.

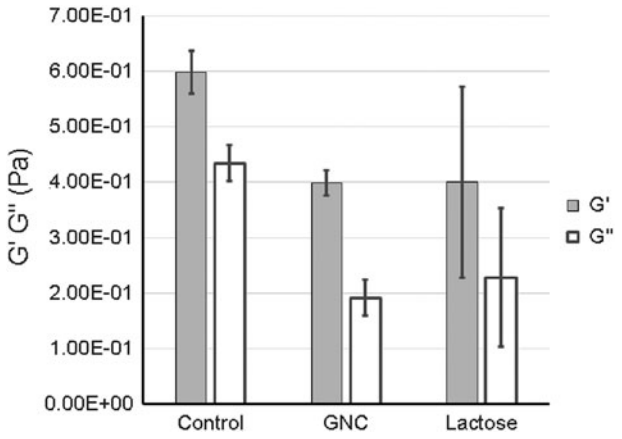

FIG. 11. Elasic moduli (G') and viscous moduli (G'') complex viscosity of 3% HBE mucus treated with 1:10 volume ratio of control buffer (0.9% NaCl, 10 mM EDTA, 0.01% sodium azide), 50 mg/mL GNC (Gem-GNC), and 40 mg/mL lactose. Results are shown as mean ± SD ($n = 3$).

mobility of nanoparticles and thus faster penetration through the mucus layer. The elastic (G') and viscous (G'') moduli decreased by 33% and 50%, respectively, from $G' = 0.60$ Pa and $G'' = 0.43$ Pa to 0.40 and 0.19 Pa, as shown in Figure 11. Lactose reduced the complex viscosity of mucus by a similar amount, but the results were too heterogeneous to ascribe statistical significance to the reduction.

Discussion

Cancer is the leading cause of death in the United States, with lung cancer contributing to the highest number of estimated cancer deaths.[4] Current treatments for lung cancer include surgery, chemotherapy, and radiation therapy. However, surgery does not completely remove the cancer in most patients, while radiotherapy and chemotherapy cause severe adverse effects and low response rates.[84,85] A nanocarrier-mediated delivery of a chemotherapeutic agent to the lung cancer tumor mass may increase the response rates and decrease the associated systemic adverse effects with conventional chemotherapeutic options. The purpose of the investigation was to formulate a Gem-GNC designed to be delivered through the inhalation route of administration and to evaluate the physical characteristics, stability, *in vitro* efficacy using A549 and H460 NSCLC cells, and aerodynamic particle size distribution.

Nanocarriers used for the delivery of Gem to cancerous tissues would allow for control of the release of the drug within local environment of the lung and avoid systemic delivery. The limitations of conventional Gem delivery are due to its low molecular weight, high hydrophilicity, short half-life (30–90 minutes), and fast decomposition to inactive products upon intravenous administration.[19] Therefore, the use of Gem-GNCs would overcome these limitations and also reduce the dose and minimize side effects.

Other methods for overcoming the limitations and increasing the efficacy of Gem include the bioconjugation of Gem with PEG and folic acid moieties, thus forming a polymeric carrier for the targeted therapy of folate receptor-expressing cancer.[86,87] Another example was the synthesis of saturated and monounsaturated C18 and C20 long-chain 4-(N)-acyl derivatives and 5I-esters of Gem (Eli Lilly and Company, Indianapolis, IN), which increased the cytotoxicity of Gem *in vitro*.[88]

Gelatin-based nanocarriers are an attractive drug delivery system since the polymer matrix that is formed during the nanocarrier formation allows for the incorporation of therapeutic cargo. There are two different types of gelatin, type A and type B. Type A is positively charged at physiological pH due to its isoelectric point in the range of 7–9 and type B is negatively charged at physiological pH since its isoelectric point is in the range of 4.7–5.4.[89,90] When preparing nanoparticles with type A gelatin, the zeta potential of the nanoparticles will be positive.[91] In contrast, preparing nanoparticles with type B gelatin will create nanoparticles with a negative zeta potential.[92] Type B gelatin has been selected for the Gem-GNC formulation. A gelatin hydrogel containing cisplatin developed by Konishi et al. illustrated sustained-release properties and resulted in an increased anticancer effect.[93]

The Taguchi method was developed by Genuchi Taguchi to improve product quality.[94] The Taguchi method is a powerful tool in the design of a high-quality system. It employs an orthogonal array design to determine the effects of the entire constitutive parameters through a smaller number of experiments. The use of the Taguchi method can allow for a reduction in the time required for experimental procedures, while being an effective means of investigating the effects of multiple factors and individual factors on a process performance.[95,96] With this method, it is possible to reduce the number of experiments required to study the influence of multiple and individual factors compared with the full factorial designs. The Taguchi orthogonal array design has been used previously to design hydrogel nanoparticle preparations comprising chitosan, gelatin, and PLGA.[97–99] The Taguchi method involves a design of experiments, followed by a technique for high-quality system design.

The selected parameters and their levels and the batch experiments and the resultant particle sizes are shown in Table 1. These effects of the levels of each factor on product quality, in this case, particle size, are defined and evaluated according to the total mean values of experimental trial results or S/N ratios. The particle size error values may be calculated by the means of total mean values of experimental trial results. Distribution of the means of S/N ratio for particle size is shown in Figure 2. For factor A, the main effects plot shows an increasing and then decreasing particle size and the opposite for the S/N ratio with increased volume ratio of 90% v/v aqueous ethanol solution (Fig. 2B). This is in accordance with the formation of small particles observed with the use of high organic solvent-to-aqueous solution ratios, imparted by the prevention of coalescence between particles due to the availability of large amounts of solvent for diffusion.[100]

The results of the second factor B, the genipin concentration (% w/w), indicate that increasing the cross-linker concentration increases particle size. At low cross-linker concentration, a nanoparticle was formed that had ideal size characteristics. For factor A, gelatin concentration (% w/v), the main effects plot (Fig. 2A, B) show increased particle size and decreased S/N ratio with increasing polymer

concentration. At high polymeric concentrations, the viscosity of the polymeric solution increases to the point where resistance against nanoparticles in the external aqueous phase reduces the Gem-GNC dispersion efficiency. This results in larger particles that often have higher EE% due to low diffusion of the drug from the polymeric solution to the external phase. The effects of the three factors on the particle size of the Gem-GNCs are summarized in equation 4.

Three batches were prepared using the optimized parameters to evaluate the model and to determine interbatch variability. The three batches showed nonsignificant ($p < 0.05$) differences in particle size and zeta potential before and after lyophilization (Table 2). There was a slight increase in particle size when comparing the Gem-GNC with the placebo GNC, possibly due to the entrapment of the Gem within the gelatin matrix. The decrease in zeta potential after lyophilization can be associated with slight increase in particle size and with the association of polysorbate 20 (Tween 20) with the surface of the GNC.

Gelatin-based nanoparticles have demonstrated safety and efficacy *in vitro* and *in vivo* by studies performed by Tseng et al., who developed gelatin nanoparticles containing cisplatin coated with epidermal growth factor (EGF) tumor-specific ligand that was administered by simple aerosol delivery.[48] Although this formulation was successful at encapsulating cisplatin and delivering it to the cancer tissue while not eliciting inflammation, the particles had a size of 200–300 nm, thus making them susceptible to alveolar macrophage uptake.[26,48] Another gelatin nanoparticle was developed for the targeted treatment of pancreatic cancer that involved a redox-responsive nature for the delivery of wt-p53 plasmid DNA and Gem.[101] A PLGA nanoparticle loaded with celecoxib was recently optimized by Taguchi design of experiments and evaluated for *in vitro* cytotoxicity.[99]

The morphology and particle size of the Gem-GNCs were examined using SEM and TEM, as shown in Figure 5. SEM images obtained are in agreement with other SEM images of gelatin nanoparticles.[102] Negative staining was used for contrasting the Gem-GNC from the optically opaque fluid, where the background was stained and the Gem-GNC was unstained. In TEM, opaqueness to electrons is directly related to atomic number or the number of protons. Negative stains are chosen due to their ability to scatter electrons strongly and to adsorb biological matter. The method for negatively staining a sample for TEM is a mild preparation method.

The interpretation of the morphology of the particle gives insight on the shape, structure, and size of the particles within the Gem-GNC formulation. The analysis of TEM images showed formation of homogeneous, smooth, and spherical nanoparticles with no aggregation (Fig. 5). These results are in agreement with other polymeric nanoparticle TEM images obtained from a gelatin nanoparticle formulation containing polymerized siRNA that found that the formulated nanoparticles had a particle size of $\sim$150 nm and that natural gelatin comprised 12.3 nm amorphous granules.[103]

The stability of the Gem-GNC batches was evaluated in water and DPBS at varying pH buffer solutions. The Gem-GNC shows good stability in water as inferred by the nonsignificant ($p < 0.05$) change in particle size up to 72 hours. The pathogenesis of lung cancer is partly due to accelerated oxidative stress associated with reduced airway pH.[104,105]

The pH in healthy lungs is in the range of 7.38–7.42, equal to the blood traveling through the body. However, in cancerous lungs, the pH drops to about 6.7.[106] Therefore, it was pertinent to examine the stability of the Gem-GNC under acidic pH 5.4 and 6.4 conditions, as well as at the normal physiological pH 7.4. The formulation also showed no significant change ($p < 0.05$) in particle size up to 3 days at pH 5.4, 6.4, and 7.4. A study by Menon et al. screened and compared the degradation and release from gelatin nanoparticles and other polymeric nanoparticles.[107] This study found that glutaraldehyde-cross-linked gelatin nanoparticles with particle size of 191 nm were stable in distilled deionized water, 10% v/v FBS, and in Gamble's simulated lung fluid for over 5 days, as inferred by no significant aggregation or change in particle size.[107]

Since we are delivering the Gem-GNC through the inhalation route of administration, it was necessary to evaluate the *in vitro* release in the presence of a simulated lung fluid. The alveolar region of the lungs does not contain mucus, but the viscoelastic layer in the tracheobronchial region does. There are many simulated lung fluids that are formulated for specific purposes such as artificial lysosomal fluid (pH 4.5) and Gamble's solution (pH 7.4) that are used to simulate fluid that particles would encounter after phagocytosis by alveolar and interstitial macrophages and deep interstitial fluid of the lung, respectively.[65] Other simulated lung fluids are variations of Gamble's solution, in that they mimic the extracellular lung fluids or the interstitial fluid.

The *in vitro* release of Gem from the Gem-GNC was investigated under physiological pH and within Gamble's SLF (Fig. 4). The *in vitro* release of the neat Gem solution showed complete release within 5 hours. In contrast, the Gem-GNC cross-linked with genipin showed Gem release of $\sim$30% at 24 hours in both dissolution media and displayed a biphasic release profile consisting of an initial burst release, followed by a prolonged release. Of the kinetic models that were fitted to the Gem-GNC release data within Gamble's SLF, the data best fit Weibull and Korsmeyer–Peppas with R^2 values of 0.990 and 0.983, respectively. The Weibull model is useful for comparing drug release profiles of matrix-type drug delivery, while the Korsmeyer–Peppas model has been used previously to describe release from several modified release dosage forms.[108]

The Korsmeyer–Peppas power law was utilized to elucidate the drug release mechanism.[49] A release exponent value of <0.5 represents Fickian diffusion, 0.5 to <1 represents non-Fickian diffusion, 1 represents case II transport, and >1 represents supercase II transport. The exponent values of 0.58 and 0.59 for the release within the respective DPBS and Gamble's SLF suggests non-Fickian diffusion. Thus, the main mechanisms that drive the release of Gem from the Gem-GNC are believed to be diffusion and erosion from a matrix-based nanocarrier. The Gem-GNC formulations exhibited the desired controlled release that will allow for the drug to be delivered to the tumor tissue in a constant manner.

DSC analysis can be used to analyze chemical and physical stability of the Gem and cross-linker (genipin) with the gelatin polymeric matrix. DSC may detect polymorphic structural changes within a polymeric matrix, which may give some insight on the formulation stability over time. It has been well established that melting and recrystallization curves can be associated with polymorphic changes in lipid

matrices.[109] Thus, it may determine and provide evidence of the incorporation of drugs within the nanoparticles through the examination of enthalpy changes. DSC is a thermoanalysis method that measures the heat flow associated with a change of temperature with transitions of materials as a function of time. Results from DSC may provide information on the endothermic or exothermic phenomena that occur due to physical and chemical changes or changes in heat capacity.[110]

The Gem-GNC displayed a glass transition temperature (Tg) peak of gelatin at 75°C, which suggests that the pure Gem or the excipient genipin was present within the nanoparticles as an amorphous disordered crystalline or solid solution state. It also suggests that the Gem-GNC preparation method did not affect the properties of gelatin.

XRD is necessary for the analysis of the presence of crystal structure and spacing in a polymeric lattice.[111,112] The incorporation of therapeutic agents influences the polymer structure and spacing. PXRD provides information of the patterns and crystallinity, which may be confirmed with DSC.

We have evaluated the thermal and powder diffraction characteristics using DSC and PXRD. To evaluate the interaction of Gem within the genipin-cross-linked Gem-GNC, DSC was conducted on various samples, including the lyophilized Gem-GNC, physical mixture of excipients, placebo GNC with unentrapped Gem, placebo GNC, gelatin, genipin, lactose monohydrate, and Gem (Fig. 6). The thermogram of Gem has an endothermic melting event, followed by degradation at ~290°C that was not observed in the Gem-GNC thermogram. This is in agreement with another study that found that cisplatin was molecularly dispersed within a gelatin matrix without significant changes in the physical and chemical profiles as shown by DSC thermograms of the drug-loaded nanoparticles compared with individual components.[113]

The crystalline or amorphous nature of the Gem entrapped within the gelatin matrix was investigated by comparison with the PXRD patterns of Gem (Fig. 7). A diffraction pattern that is missing the characteristic peaks for Gem or has a significant reduction in the intensity and sharpness of characteristic peaks and a change of baseline indicates more disordered state of the drug.[114] The crystalline or amorphous drug entrapped within the gelatin nanoparticle matrix was evaluated to ascertain the level and quality of Gem entrapment within the hydrophilic polymeric matrix of the polymeric nanoparticle.

The gelatin sample showed a highly disordered molecular distribution (Fig. 7A) as displayed by the lack of sharp peaks. Lactose monohydrate, Gem, and genipin (Fig. 7B, D, E) displayed sharp well-defined peaks, illustrating that they are in a highly ordered crystalline state. There is a strong reduction in characteristic peaks in the placebo GNC and Gem mixture when compared with the physical mixture, possibly due to missing lactose monohydrate and genipin crystalline peaks (Fig. 7C). The Gem-GNC shows an amorphous-like molecularly dispersed diffraction pattern that has significant reduction in most characteristic peaks of the placebo GNC and Gem mixture (Fig. 7F). These results are consistent with another study that performed PXRD analysis on self-assembled gelatin–oleic acid nanoparticles.[115] This study found that characteristic peaks that were associated with the highly crystalline pure drugs were absent in diffraction patterns for the drugs encapsulated within nanoparticles.[115]

Gelatin-based nanocarriers have been used previously to deliver chemotherapeutics to lung cancer tissue through the inhalation route of administration. For example, Tseng et al. prepared cisplatin-loaded EGF-modified GNCs for targeting cancerous cells in the lung that highly express EGF receptor (EGFR).[47] This formulation showed higher cisplatin concentration and associated cytotoxicity on A549 cells that show high EGFR expression and showed lower cisplatin concentration on HFL1 cells that have relatively lower EGFR expression. Postinhalation, nanoparticle accumulation in murine lung tissue that contains EGFR-overexpressing cells indicated that the formulation was capable of prolonged residence times within lung tumor tissue.

In another study, EGF-modified gelatin nanoparticle delivered doxorubicin through inhalation and exhibited controlled release.[49] These findings reflected dose-dependent cytotoxicity in A549 and H226 cells with IC_{50} values of 0.56 and 0.47 μg/mL, respectively.[49] *In vivo* biocompatibility of gelatin nanoparticles may be inferred by the lack of inflammatory or immune response elicited by the formulation.[116] Similar to these studies, lung tumor tissue nanoparticle accumulation of the EGF ligand surface-modified gelatin nanoparticles was observed.[49]

Aerosolized Gem delivered through inhalation has been previously investigated. When aerosolized Gem (1 and 4 mg/kg) was administered, one of four patients showed pulmonary toxicity, while no patients developed hematologic toxicity.[117] Animal studies on Gem administration by intratracheal instillation by tracheotomy (i.t.t.) or orotracheal route (i.t.o.) were performed in rats.[118] Pulmonary toxicity was evaluated by comparing lung morphology, histopathology, coefficient, wet/dry weight ratio, cells related with inflammation, and inflammatory cytokines. The i.t.t. and i.t.o. administrations displayed good absolute bioavailability and similar acute lung injury compared with intravenous route. Preclinical studies on the use of Gem aerosol in osteosarcoma-bearing dogs found that Gem aerosol formulation induced increased apoptotic effect with enhanced Fas expression against lung metastatic foci.[119]

These studies indicated that aerosolized Gem is an effective treatment for lung cancer. However, aerosol delivery of Gem still caused local and systemic side effects of bronchospasm, fatigue, vomiting, dyspnea, and cough. These adverse effects may be avoided if Gem was delivered through a sustained-release manner.

Inhalation therapy allows for the delivery of chemotherapeutics with local deposition at the target site with reduced side effects associated with systemic delivery while maximizing efficiency. Administration of 5-fluoracil, doxorubicin, paclitaxel, docetaxel, platinum analogs, cetuximab, 9-nitro camptothecin, interleukins, granulocyte-stimulating growth factor, and bavazisumab through the inhalation route has shown efficacy and safety in past studies.[60,120] In the 1980s, 5-fluorouracil (5-FU), the first chemotherapeutic agent, was studied in inhalation therapy.[121] It was shown that there were increased 5-FU concentrations within the tumor than in other tissues and that high concentrations of 5-FU were found in the main bronchus and associated lymph nodes.[122]

Furthermore, formulations of 5-FU involving lipid-coated nanoparticles or difluoromethylornithine were created to provoke a sustained release and enhance anticancer properties.[123,124] Liposomal carriers, nanoparticles, polymeric micelles, and lipid nanocapsules have proven to increase

therapeutic index of taxanes by prolonging the residence time and subsequent regional action in the lung.[125] This study indicated that the mononuclear phagocyte system attacks the colloidal drug, therefore a PEGylated lipid nanocapsule was needed to help prolong regional action. Other studies have shown increased efficacy of entrapped taxanes within the nanoparticle and linked to human albumin.[125–127] Neurotoxicity and other adverse effects were observed to be dose dependent, but were accompanied by decreased tumor size.[125] Cyclosporine A added to the paclitaxel aerosol was found to increase the anticancer efficacy of the therapy.[128] Taxane compounds when compared with doxorubicin have less toxicity to the lung parenchyma and do not exhibit the cardiotoxicity associated with doxorubicin treatment.[27,129]

Aerosolized celecoxib nanostructured lipid carriers have shown significant reduction in tumor growth alone and in combination with i.v. docetaxel against NSCLC.[35] Another example is the aerosol delivery of a diindolylmethane derivative combined with docetaxel for the treatment of lung cancer by the inhalation route.[60,73] To streamline the treatment methods for doxorubicin-inhaled chemotherapy to human subjects, protocols were created by Otterson et al.[130,131] These phase I and I/II studies showed that the aerosol treatment resulted in adverse effects, including mild bronchospasm and moderate reduction of pulmonary function.[131] Platinum analog delivery by inhalation has also been studied and was found to have similar effects as inhaled doxorubicin.[132,133]

On the forefront of targeted inhaled chemotherapy was a biotinylated EGF-modified gelatin nanoparticle that was found to increase the anticancer activity of cisplatin.[47,48,134] Lung cancer cells that overexpressed the EGF had increased uptake of the targeted gelatin nanoparticle containing cisplatin, which reduced nephrotoxicity due to the avoidance of systemic circulation.[48] Inhalable Gem formulations were found to be effective against metastatic osteosarcoma lesions in animal models.[119] Gem has been delivered by an aerosol or instillation within the lung parenchyma in patients with lung cancer and shown efficacy.[117,118] It is important to note that even though this formulation did not contain ingredients incompatible with aerosol delivery and did not induce fibrotic lesions within the lung parenchyma, the animal model treatments resulted in some deaths from pulmonary edema after aerosol administration of Gem.[135,136]

Inhaled chemotherapy is feasible if delivered by a nebulization system, as has been shown by the previously published conclusions of this treatment modality.[120,137] However, a missing link in the development of aerosol chemotherapy is the understanding of long-term adverse effects to the lung and more trials are needed to prove safety and efficacy when compared with conventional intravenous administration.

Aerodynamic particle size distribution is regarded by the FDA as a critical quality attribute (CQA). Cascade impaction measures the aerodynamic instead of the geometric size of the particles, the mass of the active pharmaceutical ingredient of the drug, and the mass of the entire emitted dose. Particle size distribution impacts inhalation delivery by determining the efficiency of particles to get to the deep alveolar region of the lung. There are different techniques of particle sizing used to analyze aerosol particles, including optical microscopy, laser light scattering, laser Doppler methods, and the cascade impactor method.

Cascade impaction does have limitation as an *in vitro* test for determination of actual aerodynamic particle size distribution. For example, the cascade impactor uses a fixed flow rate, as opposed to a variable inhalation flow rate that patients will be more likely to do; the USP throat is not a good reflection of the oropharyngeal pathway and dry powder particle may reentrain during the administration to the cascade impactor. Deposition in the cascade impactor is based on impaction with distinct cutoffs per stage, as opposed to the more *in vivo* relevant impaction, diffusion, and sedimentation over the whole lung surface lung deposition.

Drug delivery to the lungs through the inhalation route of administration does have its own set of limitations in physiological efficacy. Aerosols must reach the intended site of action to be effective. The tumor size itself is crucial for drug deposition and must not be larger than 5 cm in mass medium diameter.[138–140] Physical characteristics that impact distribution and retention of inhaled aerosols are particle size, velocity, charge, destiny, and hygroscopicity. In addition, deposition is influenced by the physiological factors of respiration rate, airway diameter, presence of excessive mucus, and respiratory volume. Therefore, the drug delivery system for administration of a therapeutic agent through the inhalation route of administration should be designed with these points in mind.

Cascade impactors may provide information on particles within the aerodynamic diameter range of 0.5–32 μm. Variables that will be determined are the total mass of drug released from the inhalation aerosol, the quantity of drug collected at each location of the cascade impactor device, the MMAD, and the GSD. The cascade impactor consists of a sampling chamber, the cascade impactor, a vacuum pump, and a flow meter. To determine the aerodynamic behavior, Gem-GNCs were suspended in water at a concentration of 25 mg/mL and delivered through a nebulizer into an Andersen Mark-II cascade impactor. The aerodynamic particle size distribution is shown in Figure 9. The Gem-GNC formulation displayed an MMAD of 1.99 ± 0.16 μm, GSD of 2.73 ± 0.16, and FPF of $75.2\% \pm 2.4\%$. These results are in good accordance with a nebulizer nanoliposomal celecoxib formulation developed recently that had an FPF, MMAD, and GSD of $\sim 76\%$, 1.6 μm, and 1.2 μm, respectively.[31]

An important parameter in inhalation delivery is the particle size distribution because it, in part, determines the efficiency of the delivery of particles to the deep alveolar region of the lung. Aerosol particles with aerodynamic diameters between 1 and 5 μm are optimal for inhalation delivery, therefore the obtained characteristics are suitable for pulmonary deposition within the respiratory zone.[141]

The gelatin nanoparticle formulation may impact the viscous and elastic moduli of airway mucus, which in turn may alter the natural mucociliary clearance. The most discerning technique for biophysical variability in human mucus, due to disease progression or drug treatment, is passive microbead rheology.[40] To determine the impact on mucus viscoelasticity, microbead rheology and data analytics were used to measure the baseline rheological properties of lung mucus and then GNC-treated mucus. We selected 1 Hz as an intermediate frequency between those associated with tidal breathing of ~ 0.25 Hz and mucociliary clearance, which is 10–15 Hz.[71] A significant ($p < 0.05$) reduction of $\sim 40\%$ for each of the elastic (G′) and viscous

moduli (G″) upon treatment with Gem-GNC compared with the normal saline control was observed. The lactose-treated samples were too heterogeneous to resolve statistically significant results.

After Gem is internalized by the cell, it is phosphorylated by deoxycytidine kinase, thereby generating the nucleotide monophosphate. The occurrence of further phosphorylation is rate limited by this first phosphorylation step. Furthermore, phosphorylation leads to the active diphosphate and triphosphate derivatives of Gem that have anticancer activity.[142] The Gem diphosphate indirectly inhibits ribonucleotide reductase, which results in the depletion of the deoxyribonucleotide pool needed for DNA synthesis.[143]

The resultant Gem triphosphosphate (dFdCTP) binds DNA polymerase and competes with the natural substrate deoxycytidine triphosphate. This single deoxynucleotide addition causes termination of the DNA helix as a result of binding another nucleotide due to steric hindrance.[144] This terminal dFdCTP and DNA complex is not recognized by normal cell repair factors, which then causes cell cycle arrest and apoptosis.[144]

In addition, Gem mediates within the cell cycle before cell proliferation between the G1 and S phases.[21] Gem blocks the *de novo* synthesis pathway and decreases the intracellular concentrations of normal deoxynucleotide triphosphate pools.[142] Therefore, Gem must be delivered to the cytoplasm of the cell following internalization. The developed Gem-GNC formulation with free surface amine groups allows for endosomal escape by eliciting the proton sponge effects that lyse the endosomal, thus releasing its contents within the cytoplasm of the cell.

Cell viability studies were performed in A549 and H460 cells lines with the use of the MTT viability assay. Time and dose dependency was studied by comparing the change in cell viability in response to Gem in the concentration range of 0.001–1000 μM and corresponding Gem-GNC concentrations at 48- and 72-hour time points. The placebo GNC treatment showed >95% viability of cells over placebo GNC concentration comparable with the Gem-GNC concentrations. This demonstrated the safety and nontoxicity of the GNC core that contained gelatin and genipin, the cryoprotectant lactose monohydrate, and the surfactant polysorbate 20. In other studies, GNCs have shown more than 90% cell viability to a nanoparticle concentration up to 1000 μg/mL and $\sim$80% cell viability at 2000 μg/mL, illustrating their biocompatibility at high concentrations.[107]

The A549 cells treated with Gem-GNCs did not achieve 50% cell kill after 48 hours, but after 72 hours, the Gem-GNCs obtained a twofold increase in the IC_{50} of Gem-GNC treatment when compared with the Gem solution. This increase of Gem-GNC IC50 from the IC50 of the Gem solution may have been due to the negative charge on the GNC. The A549 cells appeared to be more resistant to Gem solution and Gem-GNC cellular uptake at 48 hours than at 72 hours. The H460 cells treated with the Gem solution achieved IC_{50} values of 230 μM after 48 hours and 59 μM after 72 hours. H460 cells treated with the Gem-GNC formulation outperformed the Gem solution, corresponding to IC_{50} values of 41 μM at 48 hours and 5.7 μM at 72 hours that represent a 5-fold and 10-fold decrease from 48 to 72 hours ($^{**}p < 0.01$), respectively.

A previous study found IC_{50} values of nebulized Gem treatment on H460 cells to be 5.72 nM and treatment on A549 cells resulted in an IC_{50} value of 29.9 nM at 72 hours after treatment.[145] Theoretically, the negatively charged Gem-GNC has lower potential of cellular uptake in *in vitro* monolayer cell uptake studies due to electrostatic interactions between the negatively charged cellular membranes. The cell viability was decreased after a 72-hour treatment when compared with the 48-hour treatment, which inferred a dose and time dependency in both A549 and H460 cell lines. The Gem-GNCs were found to be efficacious and suitable for inhalation delivery. The characteristics of Gem-GNCs could be varied to achieve the deposition at the cancer site located in the mid, central, or peripheral regions of the lungs. The developed stable Gem-GNCs may be used for the treatment of lung cancer.

Conclusion

Stable Gem-GNCs were successfully developed for pulmonary delivery by using Taguchi Orthogonal Array Design of Experiments and regression analysis. The SEM and TEM images had shown that the developed Gem-GNCs were uniform in particle size and were of a smooth spherical morphology. DSC and PXRD of lyophilized Gem-GNCs indicated that the Gem and excipients were molecularly dispersed and amorphously configured, respectively. The Gem-GNCs exhibited non-Fickian diffusion and erosion of a matrix-based, nanocarrier-mediated controlled release of Gem, which was highly desirable for long-term efficient delivery of formulation with reduced dosing intervals. Redispersed freeze-dried Gem-GNC shows complex viscosity reduction in mucus rheology assessment. The nebulized Gem-GNC exhibited ideal MMAD, GSD, and FPF for inhalation administration.

The developed Gem-GNCs were found to be effective in protecting Gem from degradation and were able to deliver Gem within the tumor cells to exert anticancer activity. This study supports that an aerosolized GNC approach may be useful for the delivery of therapeutics to the lungs, possibly for lung cancer treatment. More studies are warranted to fully illustrate the *in vivo* efficacy and safety profile to evaluate the benefit-to-risk comparisons.

Acknowledgments

The authors acknowledge the support of the National Institute of General Medical Science of the National Institutes of Health under award number SC3GM109873 to Dr. Chougule and the National Science Foundation under awards DMS-1100281, DMS-1462992, and DMS-1412844 to Dr. Forest. The authors would like to acknowledge the 2013 George F. Straub Trust and Robert C. Perry Fund of the Hawai'i Community Foundation, Honolulu, HI, for research support on lung cancer to Dr. Chougule. The authors acknowledge Hawai'i Community Foundation, Honolulu, HI, for research support to Dr. Chougule on lung cancer, mesothelioma, and asthma projects (Leahi Fund) in 2015, 2013, and 2011, respectively. The authors acknowledge the donation from Dr. Robert S. Shirparo, MD, Dermatologist, Hilo, HI, to Dr. Chougule's laboratory in support of development of nanotechnology-based medicines.

The authors also acknowledge a seed grant to Dr. Chougule from the Research Corporation of the University of Hawai'i at Hilo, Hilo, HI, and The Daniel K. Inouye College of Pharmacy, University of Hawaii at Hilo, Hilo,

HI, for providing research start-up funds. The authors would like to thank Tina Carvalho at the Biological Electron Microscope Facility (BEMF) of the University of Hawaii at Manoa for obtaining the SEM and TEM images.

Author Disclosure Statement

The authors declare that no competing financial interests exist.

References

1. American Cancer Society: *Detailed Guide to Lung Cancer (Non-Small Cell)*. 2014. Available at www.cancer.org/cancer/lungcancer-non-smallcell/detailedguide/non-small-cell-lung-cancer-key-statistics (Last accessed October 22, 2014).
2. Control CfD, Prevention, and Statistics NCfH: CDC WONDER On-line Database, compiled from Compressed Mortality File 1999–2012. Series 20 No. 2R, 2014, 2014.
3. American Cancer Society: *Cancer Facts & Figures 2015*. American Cancer Society, Atlanta, 2015.
4. Howlader NNA, Krapcho M, Garshell J, Miller D, Altekruse SF, Kosary CL, Yu M, Ruhl J, Tatalovich Z, Mariotto A, Lewis DR, Chen HS, Feuer EJ, and Cronin KA (eds): *SEER Cancer Statistics Review, 1975–2011*. 2014. Available at http://seer.cancer.gov/csr/1975_2011/ (Last accessed March 19, 2015).
5. Reade CA, and Ganti AK: EGFR targeted therapy in non-small cell lung cancer: Potential role of cetuximab. Biol Targets Ther. 2009;3:215.
6. Hecht SS: Lung carcinogenesis by tobacco smoke. Int J Cancer. 2012;131:2724–2732.
7. Sutherland KD, and Berns A: Cell of origin of lung cancer. Mol Oncol. 2010;4:397–403.
8. Hanna JM, and Onaitis MW: Cell of origin of lung cancer. J Carcinog. 2013;12:6.
9. Marks R: Squamous cell carcinoma. Lancet. 1996;347:735–738.
10. Noguchi M, Morikawa A, Kawasaki M, Matsuno Y, Yamada T, Hirohashi S, Kondo H, and Shimosato Y: Small adenocarcinoma of the lung. Histologic characteristics and prognosis. Cancer. 1995;75:2844–2852.
11. Gao ZH, and Urbanski SJ: The spectrum of pulmonary mucinous cystic neoplasia: A clinicopathologic and immunohistochemical study of ten cases and review of literature. Am J Clin Pathol. 2005;124:62–70.
12. Pelosi G, Barbareschi M, Cavazza A, Graziano P, Rossi G, and Papotti M: Large cell carcinoma of the lung: A tumor in search of an author. A clinically oriented critical reappraisal. Lung Cancer. 2015;87:226–231.
13. Galmarini CM, Mackey JR, and Dumontet C: Nucleoside analogues and nucleobases in cancer treatment. Lancet Oncol. 2002;3:415–424.
14. Jorgensen CL, Nielsen TO, Bjerre KD, Liu S, Wallden B, Balslev E, Nielsen DL, and Ejlertsen B: PAM50 breast cancer intrinsic subtypes and effect of gemcitabine in advanced breast cancer patients. Acta Oncol. 2014;53:776–787.
15. Pauwels B, Korst AE, Lardon F, and Vermorken JB: Combined modality therapy of gemcitabine and radiation. Oncologist. 2005;10:34–51.
16. Caffo O, Fallani S, Marangon E, Nobili S, Cassetta MI, Murgia V, Sala F, Novelli A, Mini E, Zucchetti M, and Galligioni E: Pharmacokinetic study of gemcitabine, given as prolonged infusion at fixed dose rate, in combination with cisplatin in patients with advanced non-small-cell lung cancer. Cancer Chemother Pharmacol. 2010;65:1197–1202.
17. Dasanu CA: Gemcitabine: Vascular toxicity and prothrombotic potential. Expert Opin Drug Saf. 2008;7:703–716.
18. Dasanu CA, and Bockorny B: Recurrent pseudocellulitis due to gemcitabine: Underrecognized and underreported? J Oncol Pharm Pract. 2015;21:377.
19. Noble S, and Goa KL: Gemcitabine. A review of its pharmacology and clinical potential in non-small cell lung cancer and pancreatic cancer. Drugs. 1997;54:447–472.
20. Reddy LH, and Couvreur P: Novel approaches to deliver gemcitabine to cancers. Curr Pharm Des. 2008;14:1124–1137.
21. Mini E, Nobili S, Caciagli B, Landini I, and Mazzei T: Cellular pharmacology of gemcitabine. Ann Oncol. 2006;17 Suppl 5:v7–v12.
22. Moysan E, Bastiat G, and Benoit J-P: Gemcitabine versus modified gemcitabine: A review of several promising chemical modifications. Mol Pharm. 2013;10:430–444.
23. Ueno H, Kiyosawa K, and Kaniwa N: Pharmacogenomics of gemcitabine: Can genetic studies lead to tailor-made therapy? Br J Cancer. 2007;97:145–151.
24. Ritzel MW, Ng AM, Yao SY, Graham K, Loewen SK, Smith KM, Hyde RJ, Karpinski E, Cass CE, Baldwin SA, and Young JD: Recent molecular advances in studies of the concentrative Na+-dependent nucleoside transporter (CNT) family: Identification and characterization of novel human and mouse proteins (hCNT3 and mCNT3) broadly selective for purine and pyrimidine nucleosides (system cib). Mol Membr Biol. 2001;18:65–72.
25. Thorley AJ, Ruenraroengsak P, Potter TE, and Tetley TD: Critical determinants of uptake and translocation of nanoparticles by the human pulmonary alveolar epithelium. ACS Nano. 2014;8:11778–11789.
26. Garbuzenko OB, Mainelis G, Taratula O, and Minko T: Inhalation treatment of lung cancer: The influence of composition, size and shape of nanocarriers on their lung accumulation and retention. Cancer Biol Med. 2014;11:44–55.
27. Roa WH, Azarmi S, Al-Hallak M, Finlay WH, Magliocco AM, and Löbenberg R: Inhalable nanoparticles, a non-invasive approach to treat lung cancer in a mouse model. J Control Release. 2011;150:49–55.
28. Kim K, Kim JH, Park H, Kim Y-S, Park K, Nam H, Lee S, Park JH, Park R-W, and Kim I-S: Tumor-homing multifunctional nanoparticles for cancer theragnosis: Simultaneous diagnosis, drug delivery, and therapeutic monitoring. J Control Release. 2010;146:219–227.
29. Ganta S, Devalapally H, Shahiwala A, and Amiji M: A review of stimuli-responsive nanocarriers for drug and gene delivery. J Control Release. 2008;126:187–204.
30. Goel A, Baboota S, Sahni JK, and Ali J: Exploring targeted pulmonary delivery for treatment of lung cancer. Int J Pharm Invest. 2013;3:8–14.
31. Patlolla RR, Chougule M, Patel AR, Jackson T, Tata PNV, and Singh M: Formulation, characterization and pulmonary deposition of nebulized celecoxib encapsulated nanostructured lipid carriers. J Control Release. 2010;144:233–241.
32. Conti DS, Brewer D, Grashik J, Avasarala S, and da Rocha SR: Poly(amidoamine) dendrimer nanocarriers and

their aerosol formulations for siRNA delivery to the lung epithelium. Mol Pharm. 2014;11:1808–1822.
33. Kurmi BD, Kayat J, Gajbhiye V, Tekade RK, and Jain NK: Micro- and nanocarrier-mediated lung targeting. Expert Opin Drug Deliv. 2010;7:781–794.
34. Patel G, Chougule M, Singh M, and Misra A: Nanoliposomal dry powder formulations. Methods Enzymol. 2009; 464:167–191.
35. Patel AR, Chougule MB, Townley I, Patlolla R, Wang G, and Singh M: Efficacy of aerosolized celecoxib encapsulated nanostructured lipid carrier in non-small cell lung cancer in combination with docetaxel. Pharm Res. 2013; 30:1435–1446.
36. Vollrath A, Schubert S, and Schubert US: Fluorescence imaging of cancer tissue based on metal-free polymeric nanoparticles—A review. J Mater Chem B. 2013;1:1994–2007.
37. Shen S, Mao CQ, Yang XZ, Du XJ, Liu Y, Zhu YH, and Wang J: Cationic lipid-assisted polymeric nanoparticle mediated GATA2 siRNA delivery for synthetic lethal therapy of KRAS mutant non-small-cell lung carcinoma. Mol Pharm. 2014;11:2612–2622.
38. Li M, Al-Jamal KT, Kostarelos K, and Reineke J: Physiologically based pharmacokinetic modeling of nanoparticles. ACS Nano. 2010;4:6303–6317.
39. Kuzmov A, and Minko T: Nanotechnology approaches for inhalation treatment of lung diseases. J Control Release. 2015;219:500–518.
40. Hill DB, Vasquez PA, Mellnik J, McKinley SA, Vose A, Mu F, Henderson AG, Donaldson SH, Alexis NE, and Boucher RC: A biophysical basis for mucus solids concentration as a candidate biomarker for airways disease. PLoS One. 2014;9:e87681.
41. Youngren-Ortiz SR, Gandhi NS, España-Serrano L, and Chougule MB: Aerosol delivery of siRNA to the lungs. Part 1: Rationale for gene delivery systems. KONA. 2016; 33:63–85.
42. Lee W-H, Loo C-Y, Traini D, and Young PM: Inhalation of nanoparticle-based drug for lung cancer treatment: Advantages and challenges. Asian J Pharm Sci. 2015;10:481–489.
43. Maeda H, Nakamura H, and Fang J: The EPR effect for macromolecular drug delivery to solid tumors: Improvement of tumor uptake, lowering of systemic toxicity, and distinct tumor imaging in vivo. Adv Drug Deliv Rev. 2013;65:71–79.
44. Malafaya PB, Silva GA, and Reis RL: Natural-origin polymers as carriers and scaffolds for biomolecules and cell delivery in tissue engineering applications. Adv Drug Deliv Rev. 2007;59:207–233.
45. Inactive Ingredient Search for Approved Drug Products: Database. 2015. www. accessdata.fda.gov/scripts/cder/iig/index.cfm Accessed December 13, 2015.
46. Yao CH, Liu BS, Chang CJ, Hsu SH, and Chen YS: Preparation of networks of gelatin and genipin as degradable biomaterials. Mater Chem Phys. 2004;83:204–208.
47. Tseng CL, Su WY, Yen KC, Yang KC, and Lin FH: The use of biotinylated-EGF-modified gelatin nanoparticle carrier to enhance cisplatin accumulation in cancerous lungs via inhalation. Biomaterials. 2009;30:3476–3485.
48. Tseng C-L, Wu SY-H, Wang W-H, Peng C-L, Lin F-H, Lin C-C, Young T-H, and Shieh M-J: Targeting efficiency and biodistribution of biotinylated-EGF-conjugated gelatin nanoparticles administered via aerosol delivery in nude mice with lung cancer. Biomaterials. 2008;29:3014–3022.
49. Long JT, Cheang TY, Zhuo SY, Zeng RF, Dai QS, Li HP, and Fang S: Anticancer drug-loaded multifunctional nanoparticles to enhance the chemotherapeutic efficacy in lung cancer metastasis. J Nanobiotechnol. 2014;12:37.
50. Dandekar P, Venkataraman C, and Mehra A: Pulmonary targeting of nanoparticle drug matrices. J Aerosol Med Pulm Drug Deliv. 2010;23:343–353.
51. Schuster BS, Suk JS, Woodworth GF, and Hanes J: Nanoparticle diffusion in respiratory mucus from humans without lung disease. Biomaterials. 2013;34:3439–3446.
52. Zayas JG, Man GC, and King M: Tracheal mucus rheology in patients undergoing diagnostic bronchoscopy. Interrelations with smoking and cancer. Am Rev Respir Dis. 1990;141:1107–1113.
53. Deaton AT, Jones LD, Dunbar CA, Hickey AJ, and Williams DM: Generation of gelatin aerosol particles from nebulized solutions as model drug carrier systems. Pharm Dev Technol. 2002;7:147–153.
54. Tekade RK, Youngren-Ortiz SR, Yang H, Haware R, and Chougule MB: Designing hybrid onconase nanocarriers for mesothelioma therapy: A Taguchi orthogonal array and multivariate component driven analysis. Mol Pharm. 2014;11:3671–3683.
55. Balthasar S, Michaelis K, Dinauer N, von Briesen H, Kreuter J, and Langer K: Preparation and characterisation of antibody modified gelatin nanoparticles as drug carrier system for uptake in lymphocytes. Biomaterials. 2005;26:2723–2732.
56. Chiono V, Pulieri E, Vozzi G, Ciardelli G, Ahluwalia A, and Giusti P: Genipin-crosslinked chitosan/gelatin blends for biomedical applications. J Mater Sci Mater Med. 2008;19:889–898.
57. Lee EJ, Khan SA, Park JK, and Lim K-H: Studies on the characteristics of drug-loaded gelatin nanoparticles prepared by nanoprecipitation. Bioprocess Biosyst Eng. 2012;35:297–307.
58. Tekade RK, and Chougule MB: Formulation development and evaluation of hybrid nanocarrier for cancer therapy: Taguchi orthogonal array based design. BioMed Res Int. 2013;2013:18.
59. Roy R: *A Primer on the Taguchi Method*. Society of Manufacturing Engineers, Dearborn, MI, 1990.
60. Ichite N, Chougule M, Patel AR, Jackson T, Safe S, and Singh M: Inhalation delivery of a novel diindolylmethane derivative for the treatment of lung cancer. Mol Cancer Ther. 2010;9:3003–3014.
61. Chougule M, Padhi B, and Misra A: Nano-liposomal dry powder inhaler of tacrolimus: Preparation, characterization, and pulmonary pharmacokinetics. Int J Nanomedicine. 2007;2:675–688.
62. Hunter RJ: *Zeta Potential in Colloid Science: Principles and Applications.* Vol 2. Academic Press, San Diego, CA. 2013.
63. Sze A, Erickson D, Ren L, and Li D: Zeta-potential measurement using the Smoluchowski equation and the slope of the current–time relationship in electroosmotic flow. J Colloid Interface Sci. 2003;261:402–410.
64. Grunewald R, Kantarjian H, Keating MJ, Abbruzzese J, Tarassoff P, and Plunkett W: Pharmacologically directed design of the dose rate and schedule of 2′, 2′-difluorodeoxycytidine (gemcitabine) administration in leukemia. Cancer Res. 1990;50:6823–6826.
65. Marques MRC, Loebenberg R, and Almukainzi M: Simulated biological fluids with possible application in dissolution testing. Dissolution Technol. 2011;18:15–28.

66. Mendyk A, Jachowicz R, Fijorek K, Dorozynski P, Kulinowski P, and Polak S: KinetDS: An open source software for dissolution test data analysis. J Dissolution Technol. 2012;19:6–11.
67. Mitchell JP, Nagel MW, Wiersema KJ, and Doyle CC: Aerodynamic particle size analysis of aerosols from pressurized metered-dose inhalers: Comparison of Andersen 8-stage cascade impactor, next generation pharmaceutical impactor, and model 3321 aerodynamic particle sizer aerosol spectrometer. AAPS PharmSciTech. 2003;4:E54.
68. Mitchell J, Copley M, Sizer Y, Russell T, and Solomon D: Adapting the Abbreviated Impactor Measurement (AIM) Concept to Make Appropriate Inhaler Aerosol Measurements to Compare with Clinical Data: A Scoping Study with the ''Alberta'' Idealized Throat (AIT) Inlet. J Aerosol Med Pulm Drug Deliv. 2012;25:188–197.
69. Seagrave J, Albrecht HH, Hill DB, Rogers DF, and Solomon G: Effects of guaifenesin, N-acetylcysteine, and ambroxol on MUC5AC and mucociliary transport in primary differentiated human tracheal-bronchial cells. Respir Res. 2012;13:1.
70. Hill DB, and Button B: Establishment of respiratory air–liquid interface cultures and their use in studying mucin production, secretion, and function. Methods Mol Biol. 2012;842:245–258.
71. Tomkiewicz R, App E, Coffiner M, Fossion J, Maes P, and King M: Mucolytic treatment with N-acetylcysteine L-lysinate metered dose inhaler in dogs: Airway epithelial function changes. Eur Respir J. 1994;7:81–87.
72. Anderson WH, Coakley RD, Button B, Henderson AG, Zeman KL, Alexis NE, Peden DB, Lazarowski ER, Davis CW, and Bailey S: The relationship of mucus concentration (hydration) to mucus osmotic pressure and transport in chronic bronchitis. Am J Respir Crit Care Med. 2015; 192:182–190.
73. Ichite N, Chougule MB, Jackson T, Fulzele SV, Safe S, and Singh M: Enhancement of docetaxel anticancer activity by a novel diindolylmethane compound in human non-small cell lung cancer. Clin Cancer Res. 2009;15: 543–552.
74. Youngren SR, Tekade RK, Gustilo B, Hoffmann PR, and Chougule MB: STAT6 siRNA matrix-loaded gelatin nanocarriers: Formulation, characterization, and ex vivo proof of concept using adenocarcinoma cells. Biomed Res Int. 2013;2013:858946.
75. Uhrich KE, Cannizzaro SM, Langer RS, and Shakesheff KM: Polymeric systems for controlled drug release. Chem Rev. 1999;99:3181–3198.
76. Lin C-C, and Metters AT: Hydrogels in controlled release formulations: Network design and mathematical modeling. Adv Drug Deliv Rev. 2006;58:1379–1408.
77. Narayanan D, Geena M, Lakshmi H, Koyakutty M, Nair S, and Menon D: Poly-(ethylene glycol) modified gelatin nanoparticles for sustained delivery of the anti-inflammatory drug ibuprofen-sodium: An in vitro and in vivo analysis. Nanomedicine. 2013;9:818–828.
78. Singhvi G, and Singh M: Review: In-vitro drug release characterization models. Int J Pharm Stud Res. 2011;2: 77–84.
79. Das RK, Kasoju N, and Bora U: Encapsulation of curcumin in alginate-chitosan-pluronic composite nanoparticles for delivery to cancer cells. Nanomedicine. 2010;6: 153–160.
80. Jiang X, Li J, Zhang R, Zhu Y, and Shen J: An improved preparation process for gemcitabine. Organ Proc Res Dev. 2008;12:888–891.
81. Listiohadi Y, Hourigan JA, Sleigh RW, and Steele RJ: Thermal analysis of amorphous lactose and α-lactose monohydrate. Dairy Sci Technol. 2009;89:43–67.
82. Trevor SL, Butler MF, Adams S, Laity PR, Burley JC, and Cameron RE: Structure and phase transitions of genipin, an herbal medicine and naturally occurring cross-linker. Crystal Growth Design. 2008;8:1748–1753.
83. Apostolov A, Fakirov S, Vassileva E, Patil R, and Mark J: DSC and TGA studies of the behavior of water in native and crosslinked gelatin. J Appl Polym Sci. 1999;71:465–470.
84. Thompson JK, Westbom CM, and Shukla A: Malignant mesothelioma: Development to therapy. J Cell Biochem. 2014;115:1–7.
85. Ojima T, Takai Y, Yamazaki K, Kamata T, and Kanno M: [A difficult to treat case of malignant peritoneal mesothelioma with peritoneal metastasis]. Gan To Kagaku Ryoho. 2013;40:2463–2465.
86. Pasut G, Canal F, Dalla Via L, Arpicco S, Veronese FM, and Schiavon O: Antitumoral activity of PEG–gemcitabine prodrugs targeted by folic acid. J Control Release. 2008; 127:239–248.
87. Cavallaro G, Mariano L, Salmaso S, Caliceti P, and Gaetano G: Folate-mediated targeting of polymeric conjugates of gemcitabine. Int J Pharm. 2006;307:258–269.
88. Immordino ML, Brusa P, Rocco F, Arpicco S, Ceruti M, and Cattel L: Preparation, characterization, cytotoxicity and pharmacokinetics of liposomes containing lipophilic gemcitabine prodrugs. J Control Release. 2004;100:331–346.
89. Johnston-Banks F: Gelatine. In: Harris P. (ed). *Food Gels*. Springer; Elsevier Science Publishers, England. pp. 233–289, 1990.
90. Keenan TR: Gelatin. In: Mueller M., Matyjaszewski K. (eds). *Polymer Science: A Comprehensive Reference.* Vol 10. Elsevier BV, Amsterdam; pp. 237–247, 2012.
91. Saraogi GK, Sharma B, Joshi B, Gupta P, Gupta UD, Jain NK, and Agrawal GP: Mannosylated gelatin nanoparticles bearing isoniazid for effective management of tuberculosis. J Drug Target. 2011;19:219–227.
92. Azarmi S, Huang Y, Chen H, McQuarrie S, Abrams D, Roa W, Finlay WH, Miller GG, and Lobenberg R: Optimization of a two-step desolvation method for preparing gelatin nanoparticles and cell uptake studies in 143B osteosarcoma cancer cells. J Pharm Pharm Sci. 2006;9:124–132.
93. Konishi M, Tabata Y, Kariya M, Hosseinkhani H, Suzuki A, Fukuhara K, Mandai M, Takakura K, and Fujii S: In vivo anti-tumor effect of dual release of cisplatin and adriamycin from biodegradable gelatin hydrogel. J Control Release. 2005;103:7–19.
94. Taguchi G: *Introduction to Quality Engineering: Designing Quality into Products and Processes*, 1986. The Asian Productivity Organization.
95. Leysi-Derilou Y, and Antony J: A new insight into the Taguchi method. Qual Assur. 2001;9:55–62.
96. Jahanshahi M, Najafpour G, and Rahimnejad M: Applying the Taguchi method for optimized fabrication of bovine serum albumin (BSA) nanoparticles as drug delivery vehicles. Afr J Biotechnol. 2008;7:362–367.
97. Hamidi M, Azadi A, Ashrafi H, Rafiei P, and Mohamadi-Samani S: Taguchi orthogonal array design for the optimization of hydrogel nanoparticles for the intravenous

delivery of small-molecule drugs. J Appl Polym Sci. 2012; 126:1714–1724.
98. Kumar R, Nagarwal RC, Dhanawat M, and Pandit JK: In-vitro and in-vivo study of indomethacin loaded gelatin nanoparticles. J Biomed Nanotechnol. 2011;7:325–333.
99. Emami J, Pourmashhadi A, Sadeghi H, Varshosaz J, and Hamishehkar H: Formulation and optimization of celecoxib-loaded PLGA nanoparticles by the Taguchi design and their in vitro cytotoxicity for lung cancer therapy. Pharm Dev Technol. 2015;20:791–800.
100. Sonam, Chaudhary H, and Kumar V: Taguchi design for optimization and development of antibacterial drug-loaded PLGA nanoparticles. Int J Biol Macromol. 2014; 64:99–105.
101. Xu J, Singh A, and Amiji MM: Redox-responsive targeted gelatin nanoparticles for delivery of combination wt-p53 expressing plasmid DNA and gemcitabine in the treatment of pancreatic cancer. BMC Cancer. 2014;14:75.
102. Binulal N, Natarajan A, Menon D, Bhaskaran V, Mony U, and Nair S: Gelatin nanoparticles loaded poly (-caprolactone) nanofibrous semi-synthetic scaffolds for bone tissue engineering. Biomed Mater. 2012;7:065001.
103. Lee SJ, Yhee JY, Kim SH, Kwon IC, and Kim K: Biocompatible gelatin nanoparticles for tumor-targeted delivery of polymerized siRNA in tumor-bearing mice. J Control Release. 2013;172:358–366.
104. Bikov A, Lazar Z, Gyulai N, Szentkereszty M, Losonczy G, Horvath I, and Galffy G: Exhaled breath condensate pH in lung cancer, the impact of clinical factors. Lung. 2015;193:957–963.
105. Ricciardolo FL, Gaston B, and Hunt J: Acid stress in the pathology of asthma. J Allergy Clin Immunol. 2004;113: 610–619.
106. Antus B, and Barta I: Exhaled breath condensate pH in patients with lung cancer. Lung Cancer. 2012;75:178–180.
107. Menon JU, Ravikumar P, Pise A, Gyawali D, Hsia CCW, and Nguyen KT: Polymeric nanoparticles for pulmonary protein and DNA delivery. Acta Biomater. 2014;10:2643–2652.
108. Fu Y, and Kao WJ: Drug release kinetics and transport mechanisms of non-degradable and degradable polymeric delivery systems. Expert Opin Drug Deliv. 2010;7:429–444.
109. Bunjes H, and Unruh T: Characterization of lipid nanoparticles by differential scanning calorimetry, X-ray and neutron scattering. Adv Drug Deliv Rev. 2007;59:379–402.
110. Simon SL: Temperature-modulated differential scanning calorimetry: Theory and application. Thermochim Acta. 2001;374:55–71.
111. Kim Y-Y, Schenk AS, Ihli J, Kulak AN, Hetherington NBJ, Tang CC, Schmahl WW, Griesshaber E, Hyett G, and Meldrum FC: A critical analysis of calcium carbonate mesocrystals. Nat Commun. 2014;5:1–14.
112. Kulhari H, Pooja D, Shrivastava S, V GMN, and Sistla R: Peptide conjugated polymeric nanoparticles as a carrier for targeted delivery of docetaxel. Colloids Surf B Biointerfaces. 2014;117:166–173.
113. Dixit N, Vaibhav K, Pandey RS, Jain UK, Katare OP, Katyal A, and Madan J: Improved cisplatin delivery in cervical cancer cells by utilizing folate-grafted non-aggregated gelatin nanoparticles. Biomed Pharmacother. 2015;69:1–10.
114. Wildfong PL, Morley NA, Moore MD, and Morris KR: Quantitative determination of polymorphic composition in intact compacts by parallel-beam X-ray powder diffractometry II. Data correction for analysis of phase transformations as a function of pressure. J Pharm Biomed Anal. 2005;39:1–7.
115. Tran PH-L, Tran TT-D, and Lee B-J: Enhanced solubility and modified release of poorly water-soluble drugs via self-assembled gelatin–oleic acid nanoparticles. Int J Pharm. 2013;455:235–240.
116. Kaul G, and Amiji M: Tumor-targeted gene delivery using poly(ethylene glycol)-modified gelatin nanoparticles: In vitro and in vivo studies. Pharm Res. 2005;22:951–961.
117. Lemarie E, Vecellio L, Hureaux J, Prunier C, Valat C, Grimbert D, Boidron-Celle M, Giraudeau B, le Pape A, and Pichon E: Aerosolized gemcitabine in patients with carcinoma of the lung: Feasibility and safety study. J Aerosol Med Pulm Drug Deliv. 2011;24:261–270.
118. Min R, Li T, Du J, Zhang Y, Guo J, and Lu W-L: Pulmonary gemcitabine delivery for treating lung cancer: Pharmacokinetics and acute lung injury aspects in animals. Can J Physiol Pharmacol. 2008;86:288–298.
119. Rodriguez CO. Jr., Crabbs TA, Wilson DW, Cannan VA, Skorupski KA, Gordon N, Koshkina N, Kleinerman E, and Anderson PM: Aerosol gemcitabine: Preclinical safety and in vivo antitumor activity in osteosarcoma-bearing dogs. J Aerosol Med Pulm Drug Deliv. 2010;23: 197–206.
120. Zarogoulidis P, Chatzaki E, Porpodis K, Domvri K, Hohenforst-Schmidt W, Goldberg EP, Karamanos N, and Zarogoulidis K: Inhaled chemotherapy in lung cancer: Future concept of nanomedicine. Int J Nanomedicine. 2012;7:1551.
121. Tatsumura T, Yamamoto K, Murakami A, Tsuda M, and Sugiyama S: [New chemotherapeutic method for the treatment of tracheal and bronchial cancers—nebulization chemotherapy]. Gan No Rinsho. 1983;29:765–770.
122. Tatsumura T, Koyama S, Tsujimoto M, Kitagawa M, and Kagamimori S: Further study of nebulisation chemotherapy, a new chemotherapeutic method in the treatment of lung carcinomas: Fundamental and clinical. Br J Cancer. 1993;68:1146.
123. Hitzman CJ, Wattenberg LW, and Wiedmann TS: Pharmacokinetics of 5-fluorouracil in the hamster following inhalation delivery of lipid-coated nanoparticles. J Pharm Sci. 2006;95:1196–1211.
124. Hitzman CJ, Elmquist WF, Wattenberg LW, and Wiedmann TS: Development of a respirable, sustained release microcarrier for 5-fluorouracil I: In vitro assessment of liposomes, microspheres, and lipid coated nanoparticles. J Pharm Sci. 2006;95:1114–1126.
125. Koshkina NV, Waldrep JC, Roberts LE, Golunski E, Melton S, and Knight V: Paclitaxel liposome aerosol treatment induces inhibition of pulmonary metastases in murine renal carcinoma model. Clin Cancer Res. 2001;7: 3258–3262.
126. Musumeci T, Vicari L, Ventura C, Gulisano M, Pignatello R, and Puglisi G: Lyoprotected nanosphere formulations for paclitaxel controlled delivery. J Nanosci Nanotechnol. 2006;6:3118–3125.
127. Yang R, Yang SG, Shim WS, Cui F, Cheng G, Kim IW, Kim DD, Chung SJ, and Shim CK: Lung-specific delivery of paclitaxel by chitosan-modified PLGA nanoparticles via transient formation of microaggregates. J Pharm Sci. 2009;98:970–984.
128. Koshkina NV, Golunski E, Roberts LE, Gilbert BE, and Knight V: Cyclosporin A aerosol improves the anticancer

effect of paclitaxel aerosol in mice. J Aerosol Med. 2004;17:7–14.
129. Hershey AE, Kurzman ID, Forrest LJ, Bohling CA, Stonerook M, Placke ME, Imondi AR, and Vail DM: Inhalation chemotherapy for macroscopic primary or metastatic lung tumors: Proof of principle using dogs with spontaneously occurring tumors as a model. Clin Cancer Res. 1999;5:2653–2659.
130. Otterson GA, Villalona-Calero MA, Sharma S, Kris MG, Imondi A, Gerber M, White DA, Ratain MJ, Schiller JH, and Sandler A: Phase I study of inhaled Doxorubicin for patients with metastatic tumors to the lungs. Clin Cancer Res. 2007;13:1246–1252.
131. Otterson GA, Villalona-Calero MA, Hicks W, Pan X, Ellerton JA, Gettinger SN, and Murren JR: Phase I/II study of inhaled doxorubicin combined with platinum-based therapy for advanced non–small cell lung cancer. Clin Cancer Res. 2010;16:2466–2473.
132. Wittgen BP, Kunst PW, van der Born K, van Wijk AW, Perkins W, Pilkiewicz FG, Perez-Soler R, Nicholson S, Peters GJ, and Postmus PE: Phase I study of aerosolized SLIT cisplatin in the treatment of patients with carcinoma of the lung. Clin Cancer Res. 2007;13:2414–2421.
133. Zarogoulidis P, Eleftheriadou E, Sapardanis I, Zarogoulidou V, Lithoxopoulou H, Kontakiotis T, Karamanos N, Zachariadis G, Mabroudi M, and Zisimopoulos A: Feasibility and effectiveness of inhaled carboplatin in NSCLC patients. Invest New Drugs. 2012;30:1628–1640.
134. Tseng C-L, Yang K-C, Yen K-C, Wu SY-H, and Lin F-H: Preparation and characterization of cisplatin-incorporated gelatin nanocomplex for cancer treatment. Curr Nanosci. 2011;7:932–937.
135. Gagnadoux F, Pape A, Lemarie E, Lerondel S, Valo I, Leblond V, Racineux J, and Urban T: Aerosol delivery of chemotherapy in an orthotopic model of lung cancer. Eur Respir J. 2005;26:657–661.
136. Koshkina NV, and Kleinerman ES: Aerosol gemcitabine inhibits the growth of primary osteosarcoma and osteosarcoma lung metastases. Int J Cancer. 2005;116:458–463.
137. Zarogoulidis P, Darwiche K, Hohenforst-Schmidt W, Huang H, Li Q, Freitag L, and Zarogoulidis K: Inhaled gene therapy in lung cancer: Proof-of-concept for nano-oncology and nanobiotechnology in the management of lung cancer. Future Oncol. 2013;9:1171–1194.
138. Kleinstreuer C, Zhang Z, and Li Z: Modeling airflow and particle transport/deposition in pulmonary airways. Respir Physiol Neurobiol. 2008;163:128–138.
139. Kleinstreuer C, Zhang Z, and Donohue JF: Targeted drug-aerosol delivery in the human respiratory system. Annu Rev Biomed Eng. 2008;10:195–220.
140. Kolanjiyil AV, and Kleinstreuer C: Nanoparticle mass transfer from lung airways to systemic regions—part I: Whole-lung aerosol dynamics. J Biomech Eng. 2013;135:121003.
141. Byron PR: Prediction of drug residence times in regions of the human respiratory tract following aerosol inhalation. J Pharm Sci. 1986;75:433–438.
142. Heinemann V, Schulz L, Issels RD, and Plunkett W: Gemcitabine—A modulator of intracellular nucleotide and deoxynucleotide metabolism. Semin Oncol. 1995;22:11–18.
143. Paolino D, Cosco D, Racanicchi L, Trapasso E, Celia C, Iannone M, Puxeddu E, Costante G, Filetti S, Russo D, and Fresta M: Gemcitabine-loaded PEGylated unilamellar liposomes vs GEMZAR: Biodistribution, pharmacokinetic features and in vivo antitumor activity. J Control Release. 2010;144:144–150.
144. Huang P, Chubb S, Hertel LW, Grindey GB, and Plunkett W: Action of 2′,2′-difluorodeoxycytidine on DNA-synthesis. Cancer Res. 1991;51:6110–6117.
145. Gagnadoux F, Leblond V, Vecellio L, Hureaux J, Le Pape A, Boisdron-Celle M, Montharu J, Majoral C, Fournier J, Urban T, Diot P, Racineux J-L, and Lemarié E: Gemcitabine aerosol: *In vitro* antitumor activity and deposition imaging for preclinical safety assessment in baboons. Cancer Chemother Pharmacol. 2006;58:237–244.

Received on December 31, 2015
in final form, January 11, 2017

Reviewed by:
Zhengrong Cui
Heidi Mansour

Address correspondence to:
Mahavir B. Chougule, BPharm, MPharm, PhD
Translational Drug and Gene Delivery Research (TransDGDR) Laboratory
Department of Pharmaceutics and Drug Delivery
School of Pharmacy
Faser Hall
The University of Mississippi
University, Oxford, MS 38677

E-mail: chougule@olemiss.edu;
mahavirchougule@gmail.com